

Possible scenarios for eccentricity evolution in the extrasolar planetary system HD 181433

Giammarco Campanella^{1*}, Richard P. Nelson¹ and Craig B. Agnor¹

¹*Astronomy Unit, School of Physics and Astronomy, Queen Mary University of London, Mile End Road, London E1 4NS, U.K.*

Accepted 2013 May 31. Received 2013 May 30; in original form 2012 December 22

ABSTRACT

We analyse the dynamics of the multiple planet system HD 181433. This consists of two gas giant planets (bodies c and d) with $m \sin i = 0.65 M_{\text{Jup}}$ and $0.53 M_{\text{Jup}}$ orbiting with periods 975 and 2468 days, respectively. The two planets appear to be in a 5:2 mean motion resonance, as this is required for the system to be dynamically stable. A third planet with mass $m_b \sin i = 0.023 M_{\text{Jup}}$ orbits close to the star with orbital period 9.37 days. Each planet orbit is significantly eccentric, with current values estimated to be $e_b = 0.39$, $e_c = 0.27$ and $e_d = 0.47$. In this paper we assess different scenarios that may explain the origin of these eccentric orbits, with particular focus on the innermost body, noting that the large eccentricity of planet b cannot be explained through secular interaction with the outer pair. We consider a scenario in which the system previously contained an additional giant planet that was ejected during a period of dynamical instability among the planets. N-body simulations are presented that demonstrate that during scattering and ejection among the outer planets a close encounter between a giant and the inner body can raise e_b to its observed value. Such an outcome occurs with a frequency of a few percent. We also demonstrate, however, that obtaining the required value of e_b and having the two surviving outer planets land in 5:2 resonance is a rare outcome, leading us to consider alternative scenarios involving secular resonances. We consider the possibility that an undetected planet in the system increases the secular forcing of planet b by the exterior giant planets, but we find that the resulting eccentricity is not large enough to agree with the observed one. We also consider a scenario in which the spin-down of the central star causes the system to pass through secular resonance. In its simplest form this latter scenario fails to produce the system observed today, with the mode of failure depending sensitively on the rate of stellar spin-down. For spin-down rates above a critical value, planet b passes through the resonance too quickly, and the forced eccentricity only reaches maximum values $e_b \simeq 0.25$. Spin-down rates below the critical value lead to long-term capture of planet b in secular resonance, driving the eccentricity toward unity. If additional short-period low mass planets are present in the system, however, we find that mutual scattering can release planet b from the secular resonance, leading to a system with orbital parameters similar to those observed today.

Key words: planetary systems, dynamical evolution and stability, celestial mechanics, stars: individual: HD 181433 – methods: N-body simulations, numerical.

1 INTRODUCTION

Discovery of the first extrasolar planet around a sun-like star, 51 Peg b (Mayor & Queloz 1995), and subsequent detection of more than 850 exoplanets raises many questions about the formation and dynamics of planetary systems.

Now that we know of more than 120 multi-planet systems¹, a broad range of planetary system architectures have been sampled. This variegated ensemble offers a wide range of features that are not displayed by our Solar System: giant planets in short period orbits (“hot Jupiters”), the wide eccentricity distribution of exoplanets, the relatively common

* E-mail: g.campanella@qmul.ac.uk

¹ “The Extrasolar Planets Encyclopaedia” <http://www.exoplanet.eu>

detection of mean motion resonances (MMRs) in multiple planet systems offer interesting examples against which theories of planetary formation and evolution need to be tested (e.g. Butler et al. 2006).

Determining the physical processes that lead to the observed diversity of planetary systems remains an area of active research and debate. The discovery of dynamically quiescent, short-period multiplanet systems by the Kepler mission, such as Kepler 11 (Lissauer et al. 2011), provides clear evidence for disc-driven type I migration (Ward 1997) of bodies that probably formed beyond the ice line in their protoplanetary discs. Similarly, giant planet systems in 2:1 mean-motion resonance such as GJ 876 (Marcy et al. 2001) provide evidence for disc-driven type II migration of gap-forming planets because of the slow convergent migration rates required for resonant capture (Snellgrove et al. 2001; Lee & Peale 2002; Crida et al. 2008), as do giant planets on short to intermediate period orbits that are too remote from their central stars to have undergone significant tidal evolution.

The relatively large eccentricities observed for the extrasolar planet population as a whole, however, indicate that disc-planet interactions do not tell the whole story. A plausible explanation for many of these systems is that they formed on near-circular orbits in the disc, but after disc dispersal dynamical instability led to planet-planet gravitational scattering (Ford & Rasio 2008). Evidence is provided by the fact that numerical planet scattering experiments can reproduce the observed eccentricity distribution successfully (Chatterjee et al. 2008; Jurić & Tremaine 2008), and the observation that a number of short-period transiting planets have orbit planes inclined significantly with respect to the stellar equatorial plane (Winn et al. 2010). Further ideas for explaining eccentric orbits include eccentricity driving through disc-driven migration of a resonant pair of planets (Moorhead & Adams 2005), and sweeping secular resonances caused by various combinations of protoplanetary disc dispersal, spin-down of an initially rapidly spinning oblate central star, and general relativistic precession (Nagasawa et al. 2005; Adams & Laughlin 2006).

The three-planet extrasolar system HD 181433 has an architecture that makes it an interesting test-bed for exploring dynamical processes during and after planetary system formation. Bouchy et al. (2009) report that the system consists of two outer gas giant planets (‘*c*’ and ‘*d*’) on eccentric orbits with periods 962 ± 15 and 2172 ± 158 days, and an inner super-Earth on a 9.3743 ± 0.0019 day orbit with eccentricity $e_b = 0.396 \pm 0.062$. Dynamical analysis of this system indicates that the parameters reported by Bouchy et al. (2009) lead to global instability on very short time scales (Campanella 2011). Long-term stability requires the two outer planets to be in 5:2 mean motion resonance. Parameters that lead to a minimum χ^2_{red} value of 4.96 for the orbital fits to the data are given in table 1, and these are the parameters of the system that we adopt in this paper. It is noteworthy that planet *b* is dynamically isolated from the outer planets such that gravitational interaction over secular time scales is unable to excite the observed eccentricity of this body.

The best fit parameters presented in Campanella (2011) and reported in table 1 lead to the 5:2 resonant angles librating with large amplitude. Disc driven migration scenar-

ios for resonant capture of giant planets normally result in capture in low-order resonances with relatively small libration amplitudes (Nelson & Papaloizou 2002). Planet-planet scattering, however, may also result in resonant capture into higher order resonances with large libration amplitudes (Raymond et al. 2008), and this would appear to be a more probable explanation for the currently inferred orbital parameters for the two outer planets *c* and *d*.

In this paper, we present a case study of the evolution of the planetary system around HD 181433, and explore plausible scenarios of how the observed large eccentricities may have been generated after depletion of the protoplanetary disk. In particular we focus on scenarios that can lead to the current observed orbital configuration of planet *b*. In Section 2, we discuss the properties of the HD 181433 system, and study the locations of secular resonances and regions of stability. In Section 3, we consider how tides may have influenced the evolution of the semi-major axis and eccentricity of planet *b* over the life-time of the system. In Section 4, we explore the planet-planet scattering mechanism as a means of generating large eccentricities. We simulate the evolution in the presence of an additional giant planet whose role is to destabilise the system. We estimate the probability for planets *c* and *d* to be captured into the 5:2 MMR after scattering, and thus consider the joint probability for both resonant capture into 5:2 and excitation of the eccentricity of planet *b*. In Section 5, we examine an alternative scenario in which sweeping of secular resonances induced by stellar spin-down force the eccentricity of HD 181433*b*. We study a range of initial stellar rotation periods and spin-down rates, and examine the effect of including additional terrestrial planets – whose presence we find to be necessary for the model to be successful. In Section 6 we briefly discuss and summarize our findings.

2 PROPERTIES OF THE HD 181433 SYSTEM

The mass of the host star is reported to be $M_* = (0.781 \pm 0.10)M_\odot$ (Sousa et al. 2008), its inferred radius is $R_* = (1.01 \pm 0.07)R_\odot$ (Torres et al. 2010), while an age of (6.7 ± 1.8) Gyr has been reported (Trevisan et al. 2011). HD 181433 is believed to be of spectral type K3IV, and has a spin period of 54 days (Bouchy et al. 2009). The orbital elements of the HD 181433 planets adopted in this paper are shown in Table 1. These values are quoted from the best-fit orbital solution that is dynamically stable obtained by Campanella (2011).

The orbital period of HD 181433*b* is 9.4 days with an eccentricity of 0.39. The longitude of HD 181433*b*’s periastron advances mostly due to the relativistic correction of the Newtonian potential. Being a close-in planet in eccentric orbit, HD 181433*b* is undergoing tidal circularization. Given the age of the system and the measured $m \sin i$ value, this suggests that planet *b* has a tidal Q factor substantially larger than inferred for terrestrial planets in the Solar System, for which $Q \sim 100$ (e.g. Murray & Dermott 1999). This point is discussed further in Section 3.

The orbital parameter values quoted in Table 1 are specific to a particular moment in time. In fact, resonant and secular interactions cause e_c and e_d to reach values as large as 0.52 and 0.50, respectively (Campanella 2011). In this

Table 1. Orbital and physical parameters of HD 181433 planets.

Parameter	HD 181433 b	HD 181433 c	HD 181433 d
P (days)	9.37	975	2468
T_{peri} (BJD-2450000)	2788.92	2255.6	1844
e	0.39	0.27	0.47
ϖ ($^{\circ}$)	202.04	22	319
$m \sin i$ (M_{Jup})	0.023	0.65	0.53
$m \sin i$ (M_{\oplus})	7.4	208	167
a (AU)	0.080	1.77	3.29

paper, when discussing the eccentricities acquired by planets during dynamical evolution we will report the maximum values acquired during numerical computations once final stable systems have been established.

2.1 Formation and evolution scenarios

Before embarking on a detailed examination of the HD 181433 system, it is useful to present a qualitative description of the possible formation and evolution history. We envisage that the planets formed within a protoplanetary disc exterior to the snow-line. Planet *b* appears to have characteristics of a Neptune-like planet based on analysis of its tidal evolution (see later in the paper). It seems likely that this body formed largely from material beyond the snow-line and migrated in by type I migration, arriving at its observed location on a near-circular orbit. It is possible that it accreted during migration, possibly through giant impacts with other large bodies. If these occurred after migration was essentially complete then the body would be close to the star and the impactors would need to be at least as massive as the inferred minimum mass of *b* to generate significant eccentricity through scattering during the giant impacts phase. Interactions and giant impacts with bodies in the Earth-mass regime at semi-major axes ~ 0.1 AU would lead to $e_b < 0.1$. Therefore, we anticipate that planet *b* was formed with a small free eccentricity.

We anticipate that the outer giant planets *c* and *d* formed somewhat later than planet *b*, but were able to grow larger cores that enabled rapid gas accretion and formation of gas giant planets. Although disc driven migration may have brought the planets into close proximity, it is unlikely that it was responsible for establishing the 5:2 resonance. Disc-driven resonant locking tends to cause the resonant angles to librate with small amplitudes because the planets are pushed deep into the resonance, but planets *c* and *d* appear to be weakly embedded in the resonance (Campanella 2011). Furthermore, Nelson & Papaloizou (2002) undertook a study of disc-driven resonant capture and only obtained a 5:2 resonance when one of the two planets already had a high eccentricity equal to 0.3. A more plausible explanation for the resonance is capture as a result of planet-planet scattering, possibly involving an additional planet that was ejected during the dynamical instability (Raymond et al. 2008). Given the stabilisation provided by the eccentricity damping influence of the gas disc, this instability most likely occurred during the final stages of the disc life time or after it was dispersed altogether.

The rest of this paper largely concerns the question of how planet *b*'s eccentricity was excited, and when addressing this we consider the following possibilities: scattering by a giant planet during the previously mentioned dynamical instability that created the 5:2 resonance; by invoking the presence of an additional undetected planet in the system that enhances the forced eccentricity of planet *b*; passing planet *b* through a secular resonance through the process of stellar spin-down from an initially rapidly rotating state.

2.2 Secular evolution

For the purpose of undertaking a simplified analysis of the dynamical evolution of the HD 18433 planetary system, we have implemented a Laplace-Lagrange secular model based on the discussion in chapter 7 of Murray & Dermott (1999), assuming that all planets are coplanar. Given the standard nature of this secular theory, we refer the interested reader to Murray & Dermott (1999) for description of the mathematical details. The disturbing function includes secular terms for the mutual gravitational interaction between all three planets that are second order in the eccentricities and first order in the masses. Precession due to general relativity (GR) is also included (e.g. see Adams & Laughlin 2006), but our model does not take account of the 5:2 MMR occupied by the two outer planets. Although techniques have been developed to include first-order MMRs in secular treatments of planetary system evolution (Malhotra et al. 1989; Christou & Murray 1999; Agnor & Lin 2012), this becomes significantly more involved technically for higher order MMRs because of the requirement to include terms that are higher order in the eccentricities. Our purpose here is to use the secular theory as a rough guide to the dynamics of the system, and not to accurately predict its long term evolution, so this omission is not crucial here. This point is illustrated later in the paper where we demonstrate, by means of direct numerical simulations, that the eccentricity evolution of the two outer planets maintains highly regular and periodic behaviour, reminiscent of secular evolution (see Figure 3 for example). It appears that the effect of the 5:2 MMR is rather weak, with the main influence being an alteration of the precession frequencies. The secular model, therefore, allows us to identify the existence and approximate locations of secular resonances, in addition to estimating the magnitudes of forced eccentricities experienced by additional low mass planets that may be present in the system today, or which were present in the past. All detailed analyses of the HD 181433 system dynamics undertaken in this paper use

direct numerical simulations for accurate modelling of the mutual interactions, and all firm conclusions drawn about the past and future evolution are based on those simulations.

The secular system we examine is based on the osculating orbital elements listed in Table 1. The left-hand panel of Figure 1 shows the variation of the free precession frequency A experienced by a test particle located between 0 to 9 AU. On the same diagram the three eccentricity-pericentre eigenfrequencies of the system are denoted by solid horizontal lines. They are (in descending order) $g_2 = 0.0304^\circ \text{yr}^{-1}$, $g_3 = 0.0065^\circ \text{yr}^{-1}$ and $g_1 = 0.0049^\circ \text{yr}^{-1}$. Note that in the absence of relativistic precession $g_1 = 0.0009^\circ \text{yr}^{-1}$, with the other eigenfrequencies that are largely determined by the outer planets being essentially unaffected. The intersections of the lines with the curve show where the eigenfrequencies g_i equal A , and identify the semi-major axes where large forced eccentricities can be expected. In the central panel of Figure 1, the values of the maximum forced eccentricity are shown as a function of semi-major axis. The singularities close to 0.18, 0.7, 4.7 and 6.3 AU represent locations where the value of A is equal to one of the g_i eigenfrequencies of the secular system, as anticipated above. This plot indicates that the system is more-or-less dynamically packed out to distances of ~ 7 AU, in the sense that additional planets located in the system will experience large forced eccentricities that may be destabilising. Even in the region between 0.2–0.6 AU (focus of the right-hand panel of Figure 1), where a clear minimum exists in the forced eccentricity, a value of $e_{\text{forced}} \geq 0.2$ is predicted. It is noteworthy that the habitable zone for this K3IV star is centred at ~ 0.55 AU (Campanella 2011).

2.3 Full integration of the system

We use the symplectic N-body code Mercury-6 (Chambers 1999), augmented to include the effects of GR (Quinn et al. 1991), to perform a direct integration of the system using initial conditions from Table 1. Unless stated otherwise, all simulations in this paper adopted the hybrid integrator option which utilises the second-order mixed-variable symplectic (MVS) algorithm for systems that are not strongly interacting, but switches to the Bulirsch-Stoer (BS) integrator when the minimum separation between objects ≤ 4 Hill radii. A time step of $1/20$ of the orbital period of the innermost planets is adopted for the MVS integrator, and the Bulirsch-Stoer integrator is employed with an accuracy parameter of 10^{-11} .

Figure 2 shows two integrations of the system, one including the relativistic correction and one without it, and underlines how the relativistic correction for planet b is not relevant with regard to the amplitude of e_b , even if it is important with respect to the precession period. This differs from the *vAndromedæ* system, where the forced eccentricity of the inner planet depends sensitively on whether or not the post-Newtonian force is accounted for in secular evolution (Nagasawa & Lin 2005) because of the proximity of a secular resonance.

While the loose residence of planets c and d in the 5:2 mean motion resonances introduces some short-term oscillations, the eccentricity evolution of the system over longer periods appears regular and well-described by a simple three

frequency secular model. Fourier analysis of the system’s apsidal behaviour indicates that the main effect of the 5:2 resonance is to simply modify the values of the principal precession frequencies that describe the giant planets (i.e., $g_2 = 0.0304^\circ / \text{yr} \rightarrow 0.02305^\circ / \text{yr}$ and $g_3 = 0.00652^\circ / \text{yr} \rightarrow -0.04354^\circ / \text{yr}$ making it inaccessible for resonant interaction with g_1). Figure 3 shows the evolution of the eccentricities of the HD 181433 planets retrieved from the Laplace-Lagrange secular model (left panel) and the numerical integration (right panel). The amplitudes of the eccentricity variation are very similar, while the periodicity of the eccentricity of c and d is approximately reduced of two thirds to ~ 5000 years as result of the 5:2 MMR. This illustrates the accuracy with which the secular model estimates the locations of the secular apsidal resonance, in addition to the strong regularity displayed by the full integration even though the outer two planets are in the 5:2 MMR. It is clear that the effects of the 5:2 MMR in this system are rather weak and make only a modest change to the secular behaviour, namely through shifting the precession frequencies of the outermost planet d .

2.4 Stability of an additional low mass planet

To examine the consequences for an additional low mass planet in the system arising from the large forced eccentricities predicted in Figure 1, we have performed N-body simulations that include an additional planet. We place an Earth-mass object (which would be undetectable in current radial velocity surveys) at different distances between planets b and c to check for the stability of that region. The sampling used was of 0.05 AU for semi-major axes in the range 0.15 – 0.6 AU and 0.1 AU for semi-major axes in the range 0.7 – 1.7 AU.

We find that in full N-body simulations, the secular resonance at 0.18 AU moves inward leaving the region between 0.1– 0.35 AU stable for a single body, but unstable outside of this region. In particular, for semi-major axes $a > 0.26$ AU the forced eccentricity attains values $e_{\text{forced}} \gtrsim 0.2$. Later in the paper we consider the influence of additional low mass planets, and we find that inserting two or three extra planets with at least one of them between 0.26 and 0.35 AU makes the system unstable (see Section 5.2.2).

3 TIDAL EVOLUTION

The close proximity of planet b to its host star suggest it should be undergoing tidal evolution. Tidal effects circularize planetary orbits on a time scale given by (Goldreich & Soter 1966)

$$\tau_e = \frac{4}{63} Q \left(\frac{a^3}{GM_*} \right)^{1/2} \frac{m_p}{M_*} \left(\frac{a}{R_p} \right)^5. \quad (1)$$

The value of Q calculated for rocky objects in the Solar System is of the order of 10^2 (Murray & Dermott 1999). Such a value would imply a circularization time scale of the order of 10^7 years for planet b , much shorter than any reasonable estimate for the age of the system. If we reject the hypothesis that a recent event has generated the observed eccentricity, then the tidal factor Q must be considerably greater than

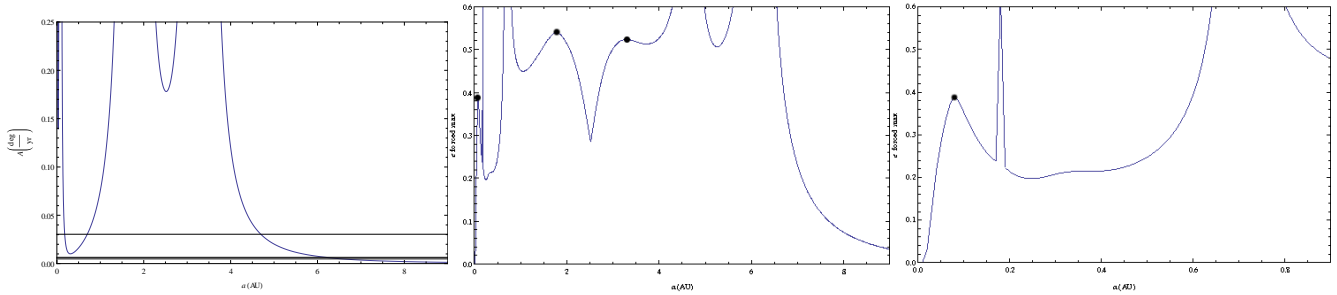


Figure 1. Secular model for the planetary system HD 181433. Left: Precession frequency A of a test particle as a function of semi-major axis, derived from perturbations by the planets and considering GR. The horizontal solid lines denote the values of the three eccentricity-pericentre eigenfrequencies. Singularities in the plot correspond to the orbital semi-major axis of the three planets. Centre: The variation in the maximum forced eccentricity as a function of semi-major axis. The dots indicate the eccentricity for the planets at their semi-major axes. The four singularities indicate regions of secular resonance where A is equal to one of the g_i . Right: The maximum forced eccentricity within 0.9 AU.

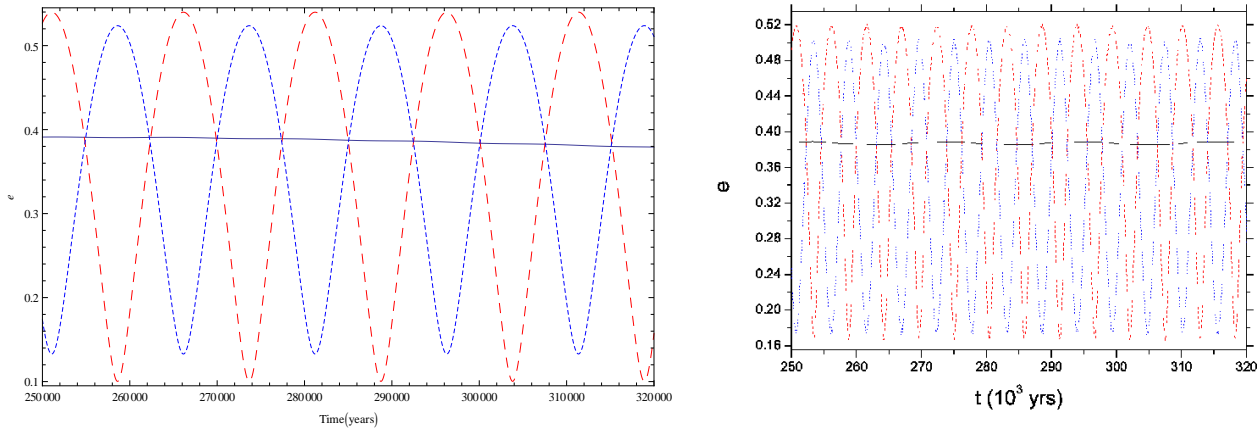


Figure 3. Eccentricity evolution of three planets around HD 181433 including the post-Newtonian effect. The solid, dashed and dotted lines show the evolution of planet b, c and d, respectively. Left: Secular model. Right: Numerical simulation.

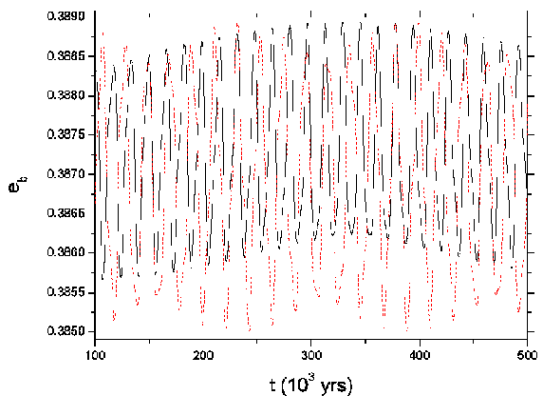


Figure 2. Eccentricity evolution of HD 181433 b . Solid line (black) not considering GR, dashed line (red) including GR.

expected for a terrestrial body of mass $\lesssim 10 M_{\oplus}$. If we assume a Q value and density typical of an ice giant such as Neptune ($Q = 10^4$, $\rho_b = \rho_{Nep} = 1.638 \text{ g cm}^{-3}$), then the circularization time scale becomes $\tau_e = 8.2 \text{ Gyr}$, comfort-

ably longer than the estimated system age. This would make HD 181433 b a member of the class of low-mass, low-density, close-in planets exemplified by Kepler 11c and Kepler 11e (Lissauer et al. 2011, 2013). To uncover the history of planet b and make an estimate for the orbital parameters that existed prior to significant tidal evolution, it is necessary to examine the influence of tides on past orbital evolution and estimate their influence of future evolution.

To study the orbital evolution of planet b we integrate the coupled tidal evolution equations for changes in a and e (see Miller et al. (2009) and references therein) backward and forward in time:

$$\frac{1}{a} \frac{da}{dt} = - \left[\frac{63\sqrt{GM_*^3 R_p^5}}{2Q_p m_p} e^2 + \frac{9\sqrt{G/M_*} R_*^5 m_p}{2Q_*} \left(1 + \frac{57}{4} e^2 \right) \right] a^{-13/2} \quad (2)$$

$$\frac{1}{e} \frac{de}{dt} = - \left[\frac{63\sqrt{GM_*^3 R_p^5}}{4Q_p m_p} + \frac{225\sqrt{G/M_*} R_*^5 m_p}{16Q_*} \right] a^{-13/2}. \quad (3)$$

The effects of the tide raised on the star Q_* as well as on the planet Q_p are both included. The stellar Q value is typically estimated through the observed circularization of binary star

orbits. The rate of tidal effects may be a very strong function of orbital frequency (Ogilvie & Lin 2004). If this is the case, the planet may spend a lot of time at certain states where tidal effects are slow and rapidly pass through states where tidal effects are faster. This model assumes that the star is rotating slowly relative to the orbit of the planet (so when the star has already evolved toward the Main Sequence) and is second order in eccentricity. It describes tidal evolution associated with orbit circularization, as this operates most rapidly, and ignores other sources of tidal interaction which operate on longer time scales. Our intention is to use this simple tidal theory to develop an approximate picture for the likely orbital history for HD 181433*b*, and its possible future evolution.

We computed the orbital evolution for various pairs of values of Q_p (ranging between 10^3 and $10^{6.5}$) and Q_* (between 10^4 and 10^7). The chosen Q values span the range that are plausible. The rate of tidal damping may depend on the interior structure of the planet and is likely to be different for different planets. We integrate the equations for the age of the star backward in time (6.7 Gyr) and for 10 Gyr into the future. Results show that only when Q_* falls below 10^4 does the behaviour change in a noticeable manner. We conduct our analysis using $Q_* = 10^{5.5}$, which corresponds to the value for which Jackson et al. (2008) have found the distribution of initial e values of close-in planets to match that of the general population. The top panel of Figure 4 shows the migration of HD 181433*b* for different values of Q_p , while in the bottom panel the evolution in $a-e$ space is presented (obtained by assuming orbital angular momentum conservation). Since both de/dt and da/dt scale $\propto a^{-13/2}$, the rate of evolution is slower for larger initial values of a , but speeds up dramatically as a decreases.

A smaller Q_p means a larger range of values is spanned during the evolution for a fixed age of the system. For example, $Q_p = 10^3$ implies that during the early main-sequence stage planet *b* would have had a semi-major axis of 0.15 AU and an eccentricity almost equal to 0.9. However, assuming a current age of 6.7 Gyr, complete circularization of the orbit will take much less than one more gigayear to be achieved (with the migration terminating at about 0.07 AU). Without further detailed information about the system allowing us to constrain its physical nature, this evolutionary track and associated Q_p value is equally probable as any others. Our purpose here is to define a plausible initial state of the system prior to significant tidal evolution, and in doing so we make the assumption that we are observing the system close to the midpoint of its tidal evolution. A value of $Q_p = 10^4$ means that planet *b* would have had initial values $a_b \simeq 0.1$ AU and $e_b \simeq 0.6$, and circularization would be completed within the next 10 Gyr. As noted earlier, $Q_p = 10^4$ is similar to the values inferred for Uranus and Neptune (Murray & Dermott 1999). We find that a value $Q_p = 10^5$ leads to tidal effects that are almost negligible such that the observed values of a_b and e_b would be very similar to those 6.7 Gyr ago. When considering mechanisms for exciting the eccentricity of planet *b*, we aim to achieve values between $0.4 \leq e_b \leq 0.6$, implying modest or essentially no tidal evolution has taken place since the excitation occurred.

For completeness, we have also investigated how the tidal evolution may depend on the actual mass of *b*. We span a range for $\sin i$ between 0.1 and 1 and we assume a

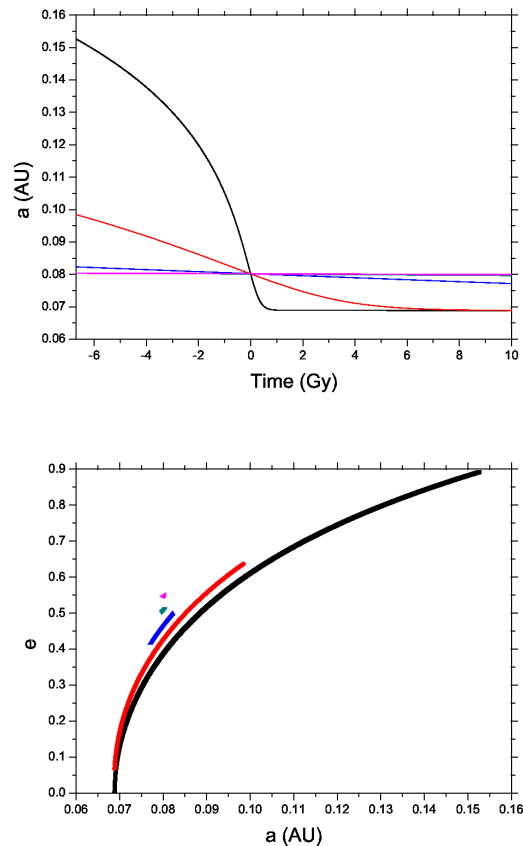


Figure 4. Tidal evolution for HD 181433*b* for the case $Q_* = 10^{5.5}$. Top panel: Orbital migration for a range of Q_p . Initially, a greater semi-major axis is expected in the case $Q_p = 10^3$, followed by the values 10^4 , 10^5 , 10^6 and $10^{6.5}$. The point of intersection between all the lines represents the present state. Bottom: Evolution in $a-e$ space for the cases Q_p equal to 10^3 , 10^4 , 10^5 , 10^6 and $10^{6.5}$. A smaller value of Q_p implies greater fraction of the $a-e$ space has been spanned. The evolution moves from right to left. For clarity, evolutionary trajectories for Q_p equal to 10^4 , 10^5 , 10^6 and $10^{6.5}$ have been off-set by $\Delta e = +0.04$ from each previous case.

density ρ_{Nep} in all cases. A smaller $\sin i$ implies a more massive planet: when $\sin i = 0.5$ planet *b* is about the mass of Uranus/Neptune. This is purely a qualitative analysis as a small $\sin i$ would imply a larger mass for planets *c* and *d* which could destabilize the system. As expected from equation 3, more massive planets experience significantly more rapid migration than less massive ones. Figure 5 displays the case for the instance $Q_p = 10^4$. In the extreme case where $\sin i = 0.1$, planet *b* should have been found initially at around 0.13 AU with an eccentricity of about 0.8; the circularization process speeds up significantly with time and would be fully accomplished in the next billion years for this particular example.

We end our discussion of tidal evolution by noting that substantial tidal heating of a gaseous planet can in principle cause it to undergo Roche lobe overflow and orbital expansion (Gu et al. 2003; Ibgui & Burrows 2009; Miller et al. 2009). As yet calculations have not been performed with pa-

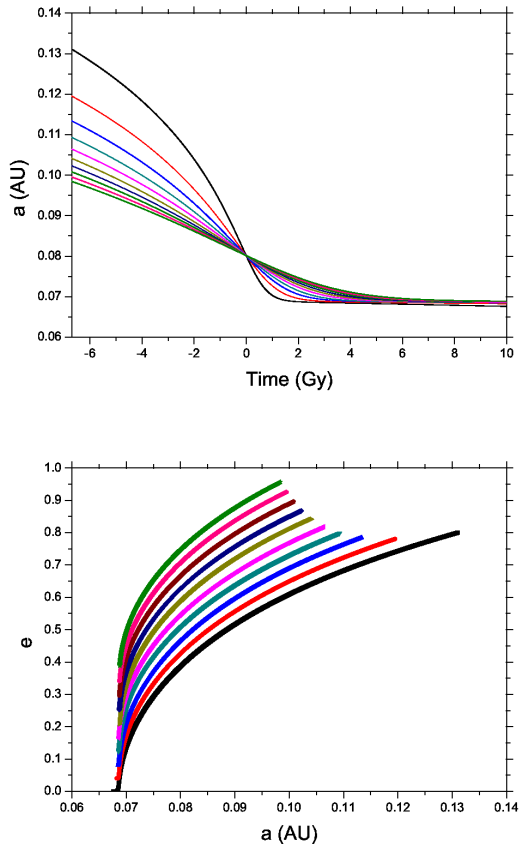


Figure 5. Tidal evolution of HD 181433*b* for the range of $\sin i$ between 0.1 and 1 when $Q_* = 10^{5.5}$ and $Q_p = 10^4$. The case $\sin i = 1$ can also be found in Figure 4. Top panel: Orbital migration. A smaller $\sin i$ corresponds to a greater initial semi-major axis and a quicker circularization. The point of intersection between all the lines represents the present state. Bottom: Evolution in $a - e$ space. A smaller value of $\sin i$ corresponds to a greater fraction of spanned space. The evolution goes from right to left. For clarity, evolutionary trajectories for values of $\sin i$ from 0.2 to 1 have been off-set by $\Delta e = +0.04$ from each previous case.

parameter sets that would allow us to determine whether or not such a scenario is compatible with the current orbital configuration of HD 181433 *b*.

4 PLANET-PLANET SCATTERING

We now consider the origin of the eccentricities of the planets in the HD 181433 system, with our primary focus being the eccentricity of the inner-most body. Recent work has demonstrated that planet-planet scattering can explain the eccentricity distribution of the extrasolar planet population as a whole (e.g. Chatterjee et al. 2008; Jurić & Tremaine 2008). Here we explore a scenario in which an additional giant planet was present in the system originally, orbiting close to the two existing outer giant planets, but shortly after dispersal of the protoplanetary disc planet-planet scattering caused this extra planet to be ejected from the system, leaving behind a three-planet system with eccentricities and semi-major axes similar to those observed today. Given the

non-linear dynamics involved, the likelihood of producing a system with parameters very close to those of the observed HD 181433 system is exceedingly small. We therefore define two requirements that must be met for a simulation outcome to be deemed a success: the inner-most planet has a close encounter with one of the giant planets during the period of dynamical instability leading to significant growth of its eccentricity; two giant planets remain at the end of the simulation in 5:2 resonance. We are able to estimate the probability of each of these separate outcomes from our simulations, and hence the joint probability of both requirements being satisfied.

We use the Mercury-6 N-body code to study this problem, and employ the hybrid integrator with the characteristics described already in Section 2.3. The physical size for the bodies is determined by their mean densities. For low mass planets we adopt a value equal to 3 g cm^{-3} , and for giant planets we adopt the Jovian value (1.326 g cm^{-3}).

4.1 Scattering between three giant planets

In order for one of the giant planets to undergo a close encounter with planet *b* and scatter it onto an eccentric orbit with $0.4 \leq e_b \leq 0.6$, as required, the perturbing body needs to have a mass large enough to generate the required velocity perturbation. The perturbing body could be the additional planet ‘*x*’ or either of the planets *c* or *d*. We approximate the eccentricity as $e \simeq v_r/v_{\text{orb}}$, where the v_r is the perturbed radial velocity and $v_{\text{orb}} = \sqrt{GM_*/a_b} = 88 \text{ km/s}$ is the Keplerian orbital velocity of *b*. Assuming that v_r due to an encounter is of the same order as the escape velocity from the perturbing planet gives $v_r \simeq \sqrt{2Gm_p/R_p}$. The mass required to generate eccentricity *e* can then be written as

$$m_p \geq e^3 v_{\text{orb}}^3 \left(\frac{3}{32\pi G^3 \rho_p} \right)^{\frac{1}{2}}$$

where ρ_p is the mean density of the perturber. Assuming a Jovian mean density gives a required mass for planet *x* in the range $0.19 \leq m_x \leq 0.64 M_{\text{Jup}}$ if it plays the role of planet *b*’s perturber. We have performed simulations with $m_x = 0.3 M_{\text{Jup}}$ which is large enough to produce values of $e_b > 0.4$. If planets *c* or *d* act as the perturbers then larger values of e_b are possible given their larger masses.

In addition to requiring that the perturbing planet can excite a large enough value of e_b , we also require that the initial conditions of our simulations at least in principle allow the observed configuration of HD 181433 to be attained once the dynamical stability has caused ejection of the additional planet. The combined specific energy of the two outer planets is given by $E_{\text{tot}} = -GM_*/(2a_c) - GM_*/(2a_d)$, and we note that ejection of planet *x* requires a loss of specific energy from the system equal to $E_x = GM_*/(2a_x)$. We therefore ensure that our initial conditions are such that if energy E_x is lost from the system of outer giant planets the remaining energy equals E_{tot} . We consider a number of basic initial configurations for our simulations, and each simulation set corresponds to a particular stellocentric ordering of the outer giant planets: *cdx*, *cx**d*, *x**cd*, *d**cx* and *x**dc*. The first and last letters in the labels correspond to the closest and further planets from the star. For each set, planet *x* is initially placed randomly between 2 and 5 mutual Hill radii

($R_{H,m} = 0.5(a_b + a_x)[(m_b + m_x)/3M_*]^{1/3}$) from its neighbour (for the set *cdx* planet *x* is initially closest to planet *d*), and the initial mean longitudes are also set randomly. The planets are initially on circular orbits with mutual inclinations $i \leq 1$ degree. We note that with the ice line defined by $a_{\text{ice}} = 2.7\sqrt{L_*/L_\odot}$ AU gives $a_{\text{ice}} = 1.50$ AU for HD 181433. Our initial set-up therefore concurs with the general expectation that giant planets emerge from the disk at locations beyond the ice line.

Throughout the integrations, close encounters and collisions between any two bodies were logged, as well as ejections and collisions with the parent star. We ran the simulations for 250 Myr but instabilities usually arise over much shorter time-scales. If dynamical instability resulted in ejection of one or more planet we calculated the orbital elements of the remaining planets. In particular, we are interested in the possibility that the two outer planets are in 5:2 resonance after the scattering, and the value attained for the eccentricity of planet *b* when the system has stabilised. In all simulations energy was conserved to a level better than 1 part in 10^4 , which is adequate for testing stability (e.g. Barnes & Quinn 2004). 300 simulations were performed overall, 50 for each of the sets described above except for set *cdx* where we ran 100 simulations.

The simulation results show that planet *x* is ejected in almost 50% of cases, but in none of our simulations do we find that planets *c* and *d* are in 5:2 mean motion resonance. The dynamical instability often leaves planets *c* and *d* more highly separated than in the observed configuration, with planet *d* in particular orbiting with significantly larger semi-major axis. Figure 6 shows the outcome from sets (*cdx*, *xcd*) that have undergone strong scattering, and we see that in each case the currently observed values of e_b , e_c and e_d are at, or close to, the upper limits of the eccentricities generated in the simulations. More importantly, these simulations also demonstrate the eccentricity of the short-period planet *b* can also be excited to the required value. Inclinations typically remain small in accordance to what was found by Ford & Rasio (2008).

The left-hand panels of Figure 7 show a case from set *cdx* where planet *x* is ejected after close encounters, and planets *c* and *d* land close to their present locations (but are not in resonance). Planets *b*, *c* and *d* achieve maximum eccentricities of 0.09, 0.29 and 0.28, respectively. A case from set *xcd* is presented in the right panels of Figure 7. Following close encounters, planet *x* is ejected with planets *c* and *d* landing at 1.6 and 4.4 AU, respectively. Planets *b*, *c* and *d* acquire maximum eccentricities of 0.19, 0.55 and 0.47, and maximum inclinations of 12° , 11° and 9° , respectively. Therefore, in this case planets *c* and *d* reach values for the eccentricities that are similar to the observed one, but planet *d* orbits at a greater distance.

A case in which e_b grows to the required value is displayed in Figure 8 where after many close encounters planet *x* is ejected and planet *b* gains a maximum eccentricity of $e_b = 0.65$, which is a value that becomes relevant when considering tidal effects (see Section 3). The final semi-major axis for planet *d*, however, is equal to 10.3 AU so the overall final architecture of the system differs considerably from the observed system. This model is also characterized by orbital inclination growth: i_b moves in the interval 25° - 83° , i_c in the range 12° - 24° , while i_d stays in the range 3° - 13° . In this

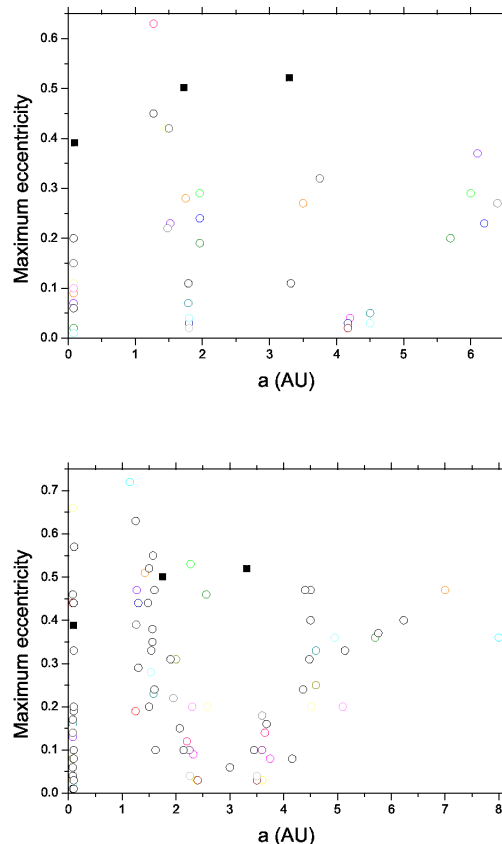


Figure 6. Comparison of our synthetic final planetary systems with the HD 181433 system showing maximum eccentricity versus semi-major axis. The values for the real planets are presented with filled black squares. Top panel: Cases from set *cdx*. Bottom: Cases from set *xcd*.

and similar cases we have checked that the large eccentricity arises because of scattering rather than the Kozai effect which can potentially become active when mutual inclinations exceed a value $\simeq 40$ degrees (Kozai 1962). Summing over all simulations, we find that 11%, 6% and 2% of the runs generate eccentricities for planet *b* of at least 0.2, 0.4 and 0.6, respectively. These simulations therefore demonstrate the feasibility of dynamical instability of the outer planet system causing all planets in the system to develop large eccentricities.

4.1.1 Probability of resonant capture

Defining a successful outcome for the planet-planet scattering experiments is not straightforward. The nonlinear nature of the process clearly means we cannot reasonably expect that a relatively small number of N-body simulations will result in systems that are close analogues to the currently-observed HD 181433 system. Instead we use a more restricted definition of success in which planet *b* experiences an increase in its eccentricity and planets *c* and *d* end up in 5:2 resonance. As discussed above, our simulations have demonstrated that the eccentricity of planet *b* can be raised to the required value, and we also have outcomes in which

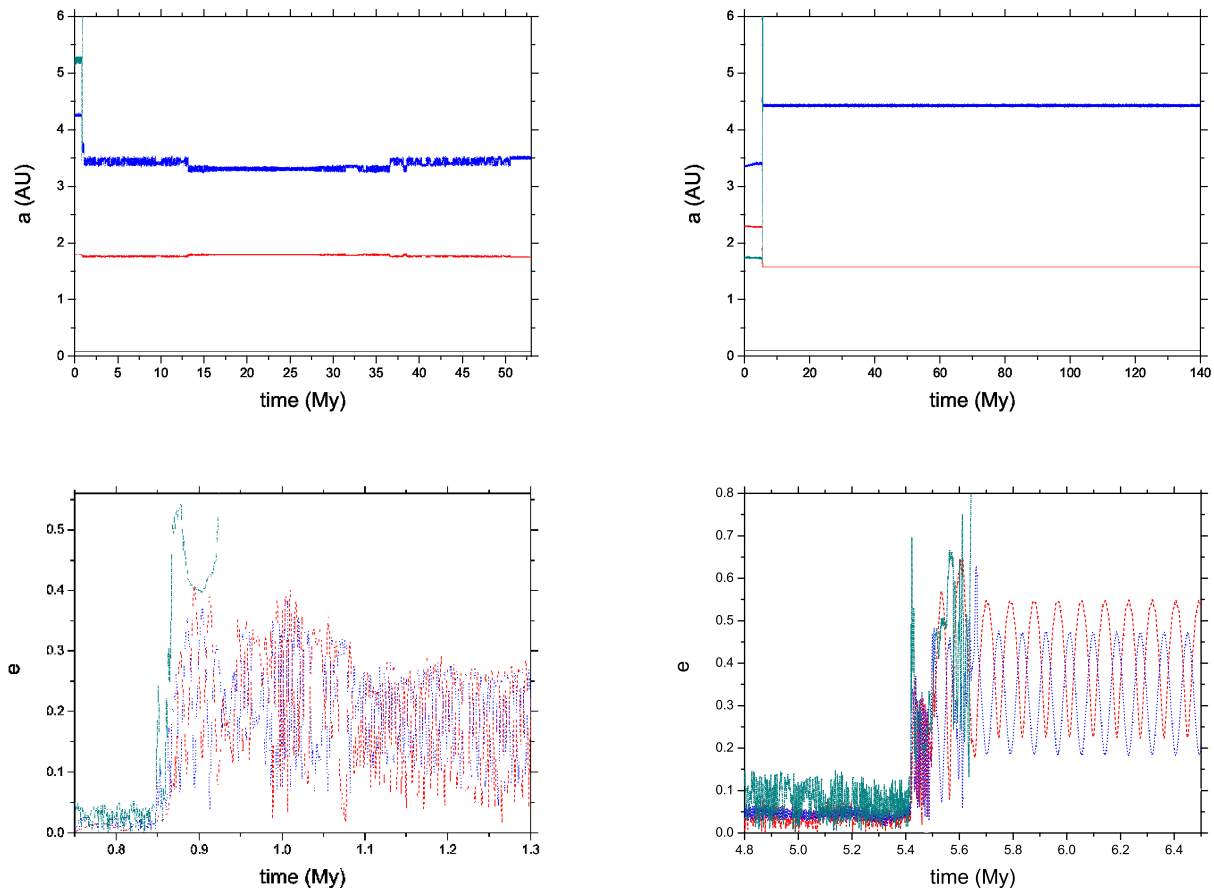


Figure 7. Evolution of a and e for two cases of scattering. Top panels: The time evolution of the semi-major axes. Initially, in order of increasing distance, we have planets b , c , d and x (left panel) and planets b , x , c and d (right panel). After ejection, the planets are in long-term stable orbits. Bottom panels: The time evolution of the eccentricities. The dashed line (red) denotes planet c , the dotted line (blue) represents planet d and the dash-dotted line (dark cyan) indicates planet x . After the ejection, the eccentricities oscillate on a secular time-scale. In the first case, e_c moves in the interval 0.03–0.29 and e_d in the range 0.05–0.28. In the second instance, e_c moves in the interval 0.22–0.55 and e_d in the range 0.18–0.47.

planets c and d have period ratios that are quite close to 5:2. None of the simulations produce a system in 5:2 resonance, however, so we now examine the probability of capture in resonance by considering the width of the 5:2 resonance and the relative mean longitudes and longitudes of pericentre required for the planets to orbit stably in resonance.

Raymond et al. (2008) show that planet-planet scattering may result in pairs of planets landing in high order MMRs. The resulting systems tend to have quite high eccentricities and resonant angles that librate with large amplitudes, characteristics that are displayed by the HD 181433 planets as described below and in Campanella (2011). The simulations presented by Raymond et al. (2008) produced a few 5:2 MMRs for every one thousand simulations. Here we examine the probability of two planets being scattered into the 5:2 MMR by determining the width of the resonance using N-body simulations that explore the dynamics of two bodies in resonance. Our procedure follows that adopted by Soja et al. (2011) in their study of asteroids in resonance. We consider the presently inferred orbital elements of planets c and d and we study the width of the region inside

of which libration occurs by varying the semi-major axis of d in steps of 0.0005 AU. For each case, we compute the maximum amplitude of the oscillations in semi-major axis by taking the difference between the maximum and minimum values over 50000 years of integration, normalized by the initial semi-major axis. The top panel of Figure 9 shows how the amplitude of oscillations in semi-major axis varies in the resonant region. Planet d survives only in the range $3.2560 \leq a \leq 3.2995$ AU, and the system is disrupted when d is placed just outside this zone. The resonant argument for the 5:2 MMR of the planetary system HD 181433 is (Campanella 2011)

$$\psi = 5\lambda_d - 2\lambda_c - 3\varpi_d \quad (4)$$

where λ is the mean longitude and ϖ is the longitude of pericentre. The bottom panel of Figure 9 shows the libration amplitude of this resonant angle as a function of the semi-major axis of planet d . The libration amplitude at the location of d that corresponds to the best-fit stable orbital solution presented by Campanella (2011) agrees well with

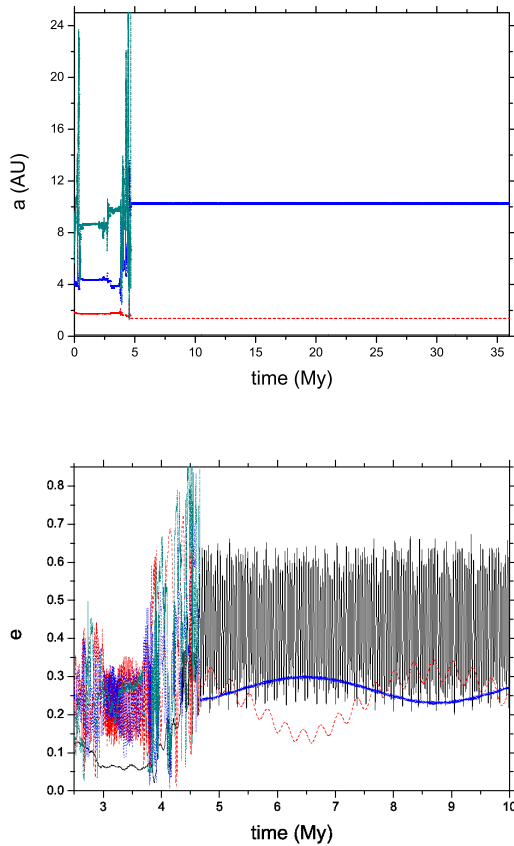


Figure 8. Evolution of some orbital elements for a configuration from set cdx. Top panel: Time evolutions of the semi-major axes. Initially, in order of increasing distance planets b , c , d and x are located. Bottom: Time evolutions of the eccentricities. The solid (black) line indicates planet b , the dashed line (red) represents planet c , the dotted line (blue) denotes planet d and the dashed-dotted line (dark cyan) is planet x . When x is ejected around 4.5 My, the eccentricities oscillate stably on a secular time-scale. e_b moves in the interval 0.20-0.65, e_c moves in the interval 0.12-0.34, while e_d in the range 0.23-0.30.

the value quoted in that paper. We find the width of the resonance to be $\Delta_a = 0.0435$ AU centred at $a = 3.2775$ AU.

A simple estimate for the probability of the planets landing within the resonance after scattering is

$$P(\Delta_a) = \frac{\Delta_a}{\overline{a_d - a_c}} \quad (5)$$

where $\overline{a_d - a_c}$ is the median value of $a_d - a_c$ at the end of all simulations for which strong planet-planet interactions occurred (we include only those runs for which final eccentricity of at least one of the planets $e > 0.1$). We obtain $P(\Delta_a) = 0.0075$. Having planets land within the required Δ_a after scattering, however, does not guarantee that they will be in resonance. It also depends on the angles that define the mutual orientation of their eccentric orbits (the difference between their longitudes of pericentre $\varpi_c - \varpi_d$), and also the values of their mean anomalies at the beginning of their interaction once they land within the resonance width. To quantify this aspect of the problem we ran a set of simulations where we take the semi-major axis values that lie

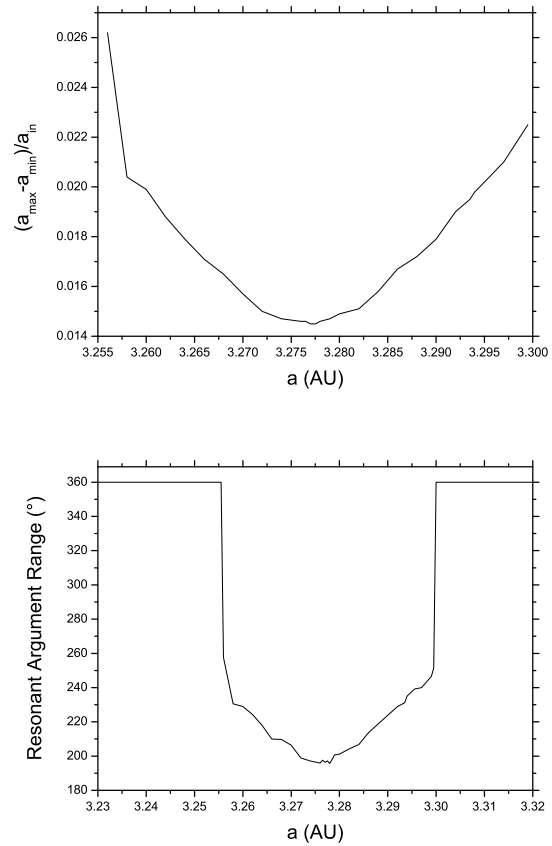


Figure 9. The width of the 5:2 MMR. Top panel: The variation in size of resonant semi-major axis oscillations for different locations of planet d . Bottom: The variation in the resonant argument. The system is unstable outside the resonance.

at the centre of the resonance, and the eccentricity values for the stable best fit solution. We vary $\varpi_c - \varpi_d$ in steps of 90° and the mean anomalies M_c and M_d in steps of 45° , for a total of 256 simulations. We ran the integrations for 30 Myr. 34 pairs of planets survive, all in resonance and in anti-aligned mode. The resonant argument (equation 4) librates with amplitudes that vary from a few degrees up to about 240° , as outlined by the lower panel of Figure 9. Finally, we are able to estimate the probability of resonance capture to be $P_{5:2} \sim 0.0075 \times 34/256 \simeq 10^{-3}$, in decent agreement with the larger sample of numerical simulations presented by Raymond et al. (2008).

4.1.2 Probability of scattering generating HD 181433 systems

We have determined that planetary systems with global structure similar to HD 181433, but which originally had an additional gas giant planet orbiting close to the two outer giant planets, can lead to the excitation of the eccentricity of the inner super-Earth up to values $e_b \simeq 0.4$ during approximately 6 % of the time when the system experiences a global dynamical instability. This eccentricity excitation occurs because one or more of the outer planets has a close encounter (or a series of close encounters) with the inner

planet during the chaotic phase of evolution. Treating the perturbation of the interior planet b onto an eccentric orbit, and the landing of the two outer planets in the 5:2 mean motion resonance, as being independent processes, the joint probability of eccentricity excitation and resonant capture becomes $P \simeq 6 \times 10^{-5}$. Taken at face value, this result suggests that systems with characteristics similar to HD 181433 occur through planet-planet scattering rather rarely.

5 SWEEPING SECULAR RESONANCES DUE TO STELLAR SPIN-DOWN

Having determined that the planet-planet scattering hypothesis is a plausible scenario for excitation of the eccentricity of all planets in the HD 181433 system, but that the excitation of e_b combined with resonant capture of planets c and d is likely to be a rare event, we now consider alternative scenarios for exciting planet b 's eccentricity. We consider the hypothesis that the eccentricities and resonant structure for the orbits of the outer planets were established after a period of dynamical instability once gas disc dispersal had occurred, and the eccentricity of planet b was established through the sweeping of a secular resonance with the outer planets caused by the spin-down of the central star from an initial state of very rapid rotation.

The idea that a short-period planet may experience excitation of its eccentricity and inclination because of stellar spin-down originates with Ward et al. (1976). They showed that if the primordial gravitational field of the Sun had a larger second-degree harmonic [i.e. $J_2 \gtrsim \mathcal{O}(10^{-3})$], equivalent to a rotation period $\lesssim 5.7$ hours, then subsequent solar spin-down would drive Mercury's orbit through secular resonances capable of generating its large mean eccentricity and inclination. Secular resonances are generated when the orbits of two bodies precess synchronously. A small body in secular resonance with a large planet will have its eccentricity and inclination modified over relatively short time periods. As the mass distribution of a planetary system evolves, for example as a result of gas disc dispersal, orbital migration or stellar spin-down, the locations of secular resonances move. Planets located in regions through which the resonance sweeps are perturbed as the resonance drives the eccentricity and inclination. Given that we assume the current orbits of the outer planets were established shortly after gas disc dispersal, stellar spin-down provides the resonant sweeping in our model, and the rate of eccentricity/inclination forcing scales with the square root of the stellar spin-down time (Nagasawa et al. 2005). In principle it should therefore be possible to tune the spin-down time scale to obtain the desired eccentricity for planet b . There are other planetary systems with architectures similar to HD 181433 (i.e., a factor of > 10 in orbit period between the inner and outer planets, and an eccentric inner planet) such as HD125612 and μ Arae. The same arguments used to constrain the orbital history of the HD 181433 system may apply to these systems too. We are investigating the more general implications of these evolutionary tuning processes and their application elsewhere (Agnor & Lin 2012).

Stars are generally believed to lose their primordial angular momentum through the magnetic braking action of the stellar wind with a mass-loss rate orders of magnitude

greater than that on the main sequence (e.g. Skumanich 1972). Pre-main sequence stars with masses over $0.25M_\odot$ exhibit a bimodal period distribution with observed values clustered around 6–8 days and 2 days. The transition between the two peaks is fairly abrupt. T Tauri stars can have spin periods of the order of hours during their evolution, with a significant fraction of them showing this characteristic (Herbst et al. 2002; Baxter et al. 2008). In addition to providing a method of exciting the eccentricity of an interior planet through resonant sweeping (Ward et al. 1976), stellar spin-down from an initial rapid state of rotation has also been invoked to explain the low eccentricity of an interior planet. Using early system parameters for the then three planet ν Andromedæ system, Nagasawa & Lin (2005) showed that the rotation period of the parent star had to be shorter than 2 days during dispersal of the gas disc so that the passage of the sweeping secular resonance near the orbit of the short-period planet b could have been avoided leaving its eccentricity at a low level. Our model differs in that we assume the eccentricities of the outer planets to have been established after gas disc removal rather than before or during its occurrence given its role in damping large planetary eccentricities (e.g. Papaloizou et al. 2001).

5.1 Secular model including stellar spin-down

We begin our analysis by modifying the Laplace-Lagrange secular model described in Section 2 to account for stellar spin-down through inclusion of the J_2 contribution to the eigenfrequencies of the system. As previously remarked, the secular model provides only an approximate estimate of the locations of secular resonance and can therefore be used to quickly evaluate the hypothesis that a secular resonance may have swept the present-day semi-major axis of planet b at 0.080 AU during stellar spin-down. We adopt the method described in Murray & Dermott (1999) for including the J_2 terms, and we use the relation between the stellar spin period P_* and J_2 provided by Ward et al. (1976).

The mass of planet b is much smaller than the outer two giants so we treat it as a test particle in the secular model. The left panel of Figure 10 presents the free precession period of a test particle induced by planets c and d . It is important to point out the role of GR-induced precession in promoting secular resonances close to the star: neglecting GR, the precession rate would fade to zero very near to the star making it difficult to match any eigenfrequencies of the outer planet secular system (see Section 2 for how precession rates change due to GR). The central and right plots in Figure 10 show the sweeping of two secular resonances as the parent star spins down from a rotation period of 2 days to 30 days (for which the J_2 effects become insignificant). According to this simplified model, when the rotation period of HD 181433 was $P_* \approx 2.1$ days (equivalent to $J_2 \approx 2.2 \times 10^{-5}$), the free precession rate at the present location of planet b matched the one of the eigenfrequencies of the system. Later, the secular resonances move inward toward their present-day locations. Using the argument that the eccentricity excitation due to the passage of a secular resonance is inversely proportional to the square root of the changing rate of the resonant frequency (Nagasawa et al. 2005), we can estimate the spin-down time $\tau = \Omega/\dot{\Omega}$, where $\Omega = 2\pi/P_*$ is the ro-

tational angular velocity of the star required to excite the present eccentricity. We have:

$$e \simeq \left(\frac{2\pi}{|\dot{A}|} \right)^{1/2} \mu_d \quad (6)$$

where, from Murray & Dermott (1999),

$$\mu_d = \sum_{j=1}^2 A_j e_{jd} \quad (7)$$

with μ_d modelling the resonance of interest, e_{jd} being the components of the scaled eigenvector for planet d , A_j defined by equation 7.142 in Murray & Dermott (1999), and \dot{A} is the rate of change of the resonant precession frequency $A = \dot{\omega}$ at resonance. Stellar rotation enhances the star's oblateness. The effect of rotation on stellar oblateness can be encapsulated in the resulting J_2 coefficient which allows for simple inclusion into secular models and N-body simulations. From Ward et al. (1976), we have:

$$J_2 = \frac{2}{3} k \frac{\Omega^2 R_*^3}{GM_*} \quad (8)$$

where for the apsidal constant k we take the value $8.16 \cdot 10^{-3}$ calculated for the Sun (Ward et al. 1976). Combining Eq.8 with secular theory for an oblate primary (Murray & Dermott 1999) gives the following relation between the spin down rate of the star $\dot{\Omega}$ and the rate of change in the precession frequency \dot{A}

$$\dot{A} \simeq 2 \left(\frac{R_*}{a} \right)^2 \left(\frac{\dot{\Omega}}{\Omega} \right) k \left(\frac{\Omega^2 R_*^3}{GM_*} \right) n. \quad (9)$$

Finally, for HD 181433 b this model suggests that a spin down timescale of $\tau \approx 1.9 \times 10^7$ years may be capable of accounting for its large observed free eccentricity of 0.39. This time scale is consistent with estimated mass loss rates from stars in the T-Tauri stage (Ward et al. 1976), suggesting that excitation of planet b 's eccentricity through sweeping secular resonances is a realistic hypothesis worthy of further more detailed exploration.

5.2 N-body simulations of secular resonance sweeping

As discussed in Section 2, the precession period for planet d is shorter than suggested by the secular model because of MMR effects. Therefore, we implement a stellar spin-down model in the BS algorithm of the integrator MERCURY-6 to account for the time dependent rotational flattening of the host star. Our model now includes effects due to GR and stellar oblateness, where we adopt the expression for the acceleration due to the oblate star given by Nagasawa & Lin (2005), in addition to the gravitational interaction between the three planets. We have run checks to ensure that the precession periods that arise from the simulations agree with analytical expression from secular theory. The stellar spin-down is modelled as a magnetic braking torque based on the empirical Skumanich law (Skumanich 1972):

$$\frac{d\Omega}{dt} = -\alpha \Omega^2 \quad (10)$$

where Ω is the stellar spin vector and $\alpha = 1.5 \times 10^{-14}$ years for a G or K dwarf (e.g., Barker & Ogilvie 2009). This pa-

rameter measures the speed of removal of angular momentum from a rotating star. Given the importance of angular momentum in determining the eccentricity evolution of the system we have confirmed that it is conserved in the simulations at a level better than 1 part in 10^6 .

5.2.1 Evolution during resonant sweeping

The secular theory suggests that a stellar spin period of between 11.1–16.7 hours would force planet b to precess with a frequency similar to one of the system's eigenfrequencies, such that a resonance may be established. For comparison, the minimum rotation period for the star is $P_{cr} = 2\pi \sqrt{R_*^3/GM_*} \approx 3.2$ hours.

We initiate N-body simulations with planets c and d in their inferred present day configuration, and with planet b on a circular orbit close to the star (later on we consider scenarios with differing implications for the long-term tidal evolution of the system discussed in Section 3, and so place planet b at different semi-major axes). Here we consider evolution that implies very little tidal evolution of the system has occurred over its life-time, consistent with an adopted value of $Q_p \gtrsim 10^5$ as discussed in Section 3. We therefore place planet b with its currently observed semi-major axis $a_b = 0.08$ AU. We initiate simulations with a stellar spin period of 14 hours, and vary the value of the spin-down parameter α , beginning with its nominal value given above.

Results are shown in the top panels of Figure 11 for the nominal value of $\alpha = 1.5 \times 10^{-14}$ years. In the right panel it is possible to observe how the relative longitudes of pericentre $\varpi_b - \varpi_c$ evolve during the process: the initial growth of eccentricity begins when the precession rates of planets b and c match ($P_* \approx 16$ hours). The passage of the resonance is anticipated by the orbit of b precessing faster initially and then being overtaken by the precession rate of c . e_b peaks at 0.16 and stabilizes later at a value of $e_b \simeq 0.13$. Setting the initial stellar rotation period to 5 hours instead of 14 hours produces the same result, with the eccentricity peaking when the stellar spin period is 17 hours.

Excitation of orbital eccentricity depends on the mass and eccentricity of the perturber. Bouchy et al. (2009) do not report an uncertainty on the mass of planet c , while the quoted errors on e_c are relatively small with $\sigma_{e_c} = 0.02$. Such a small change in the value of e_c would lead to only small changes in our results. We know the minimum mass of c . However, Campanella (2011) notes that the stable best-fit is found in a dynamically active region of phase space, and a value for $\sin i$ noticeably different from 1 would generate instabilities in the system. A slightly increased mass for planet c would lead to only a slightly modified secular resonance.

As discussed above, the expected level of eccentricity excitation depends on the rate of resonant sweeping. A larger value of e_b requires the spin-down rate to be slower, so we have examined how the evolution changes with smaller values of α . Interestingly, we find that the system behaviour can be divided into two distinct modes that depend critically on the value of α . For spin-down rates that exceed the critical value (α_{crit} is 5.75 % smaller than the nominal value) the evolution is similar to that described above and illustrated in the upper panels of Figure 11: temporary capture in the resonance and excitation of e_b to values $e_b \lesssim 0.25$.

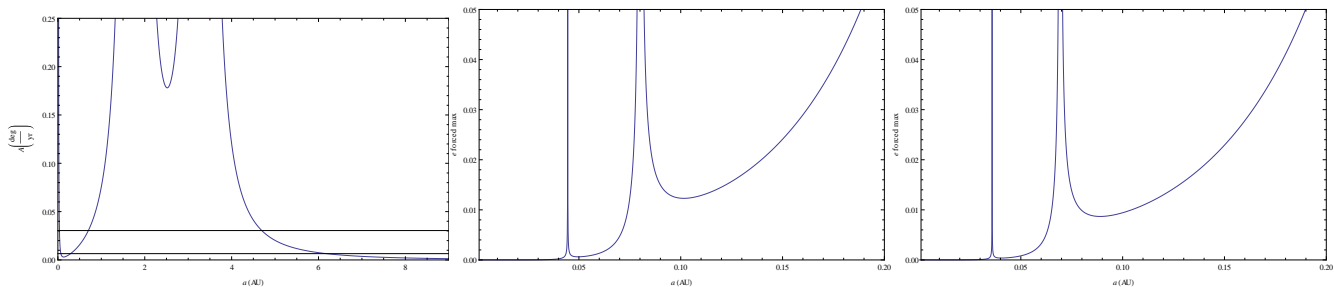


Figure 10. The process of sweeping secular resonances for HD 181433. Left: Precession frequency A of a test particle as a function of semi-major axis, derived from perturbations by the two giant planets, considering stellar spin and GR. The horizontal solid lines denote the values of the two eccentricity-pericentre eigenfrequencies. Centre: The maximum forced eccentricity in the very close region of the parent star which is assumed to rotate in 2.1 days. The secular resonances are located at 0.045 and 0.08 AU. Right: The maximum forced eccentricity within 0.2 AU from HD 181433 when it is slowly rotating. The secular resonances have now moved to 0.035 and 0.07 AU, respectively.

Spin-down parameters equal to or smaller than α_{crit} lead to long-term capture in the secular resonance (apparently indefinite capture) and growth of e_b toward unity. This mode of evolution is shown in the lower panels of Figure 11 for a run with $\alpha = \alpha_{\text{crit}}$, where over a run time of 18 Myr e_b reaches a value of 0.7 and $\varpi_b - \varpi_c$ librates around zero with a semi-amplitude of ~ 45 degrees. Apparently a planet caught within this mode of evolution is driven to $e_b = 1$ and collision with the central star unless tides are able to intervene for cases where Q_p is small enough to drive sufficiently rapid tidal damping of e_b .

The reason for the existence of these two regimes can be sought in the expressions for the precession rate of the longitude of periastron due to GR and J_2 , $\dot{\varpi}_{GR}$ (see e.g. Misner et al. 1973 for a derivation) and $\dot{\varpi}_{J_2}$ (Iorio 2005), respectively:

$$\dot{\varpi}_{GR} = \frac{3GM_*}{ac^2(1-e^2)}n \quad \dot{\varpi}_{J_2} = \frac{3}{2} \frac{J_2}{(1-e^2)^2} \left(\frac{R_*}{a}\right)^2 n \quad (11)$$

where n is the mean motion, and both $\dot{\varpi}_{GR}$ and $\dot{\varpi}_{J_2}$ depend on the eccentricity such that an increase in e leads to an increase in $\dot{\varpi}_{GR}$ and $\dot{\varpi}_{J_2}$. The condition for the resonance to be maintained during spin-down is given by

$$\frac{\partial \dot{\varpi}_{J_2}}{\partial J_2} \frac{dJ_2}{dt} = - \left(\frac{\partial \dot{\varpi}_{J_2}}{\partial e} + \frac{\partial \dot{\varpi}_{GR}}{\partial e} \right) \frac{de}{dt}. \quad (12)$$

In other words, the reduction in precession rate due to stellar spin-down needs to be compensated by the increase in precession rate that occurs as eccentricity grows. We predict from equation 12 that removing the effects of GR will still allow long term secular resonant locking, but for slower values of the spin-down parameter α . We have performed simulations to examine this by omitting the GR term in the equations of motion, and find that a rotation period of $\simeq 15$ hours is required to enter secular resonance and the spin-down parameter needs to be more than 20 % smaller than the nominal value to maintain long-term resonant capture, in agreement with our expectation. The plots in Figure 12 show the growth of e_b for different values of α in cases in which GR effects are included (left panel) and neglected (right panel), demonstrating long-term resonant capture for α below a threshold value in each case.

5.2.2 Resonant sweeping with additional exterior planets

The simulations presented in the previous section indicate two modes of behaviour, but neither of them are able to explain the observed eccentricity of planet b . One results in an eccentricity that is too small, and the other apparently results in either an eccentricity which is too high or collision with the central star. One possibility that we explore here is that there may have been additional planets in the system orbiting relatively close to planet b during sweeping of the secular resonance. If the spin-down is below the critical value required for long-term capture then interactions with the additional planets when the eccentricity becomes large may release planet b from the secular resonance, resulting in a final eccentricity of the required magnitude.

We begin by exploring the evolution with one additional Earth-mass planet (so-called planet x) in the system located outside of the orbit of planet b on a circular orbit. We ran a suite of 12 simulations where planet x is located within 2-8 mutual Hill radii from the apocentre of planet b calculated when e_b is in the range 0.3-0.7. The idea here is to induce planet-planet scattering when eccentricity growth is already underway; it is equivalent to placing planet x in the range 0.10-0.16 AU. Including planet x modifies the resonance condition, so for each simulation we have calculated the new spin period required to produce the necessary precession rate for b . We find that for an additional Earth-mass planet placed between 0.10-0.16 AU, that a stellar spin period from 0.75 days up to 5 days will enable resonant interaction with the exterior giants during stellar spin down.

The simulations yield the result that both planets b and x become trapped in the secular resonance with c , and each of them experiences eccentricity growth without limit. Figure 13 reports one example with planet x at 0.14 AU, a stellar spin period $\simeq 20$ hours necessary to generate the resonance, and spin-down parameter α that is 6% smaller than the nominal value. The left panel illustrates how the orbits of b and x cross as their eccentricities grow continuously (central plot). Collisions are avoided, however, because planet x is trapped in resonance with planet b , as demonstrated by the right panel. Planets b and c are in a secular apsidal resonance, with $\varpi_b - \varpi_c$ librating around 0° with a semi-amplitude of $\sim 45^\circ$. This behaviour is a feature of all runs for which we included one additional Earth-mass planet, and

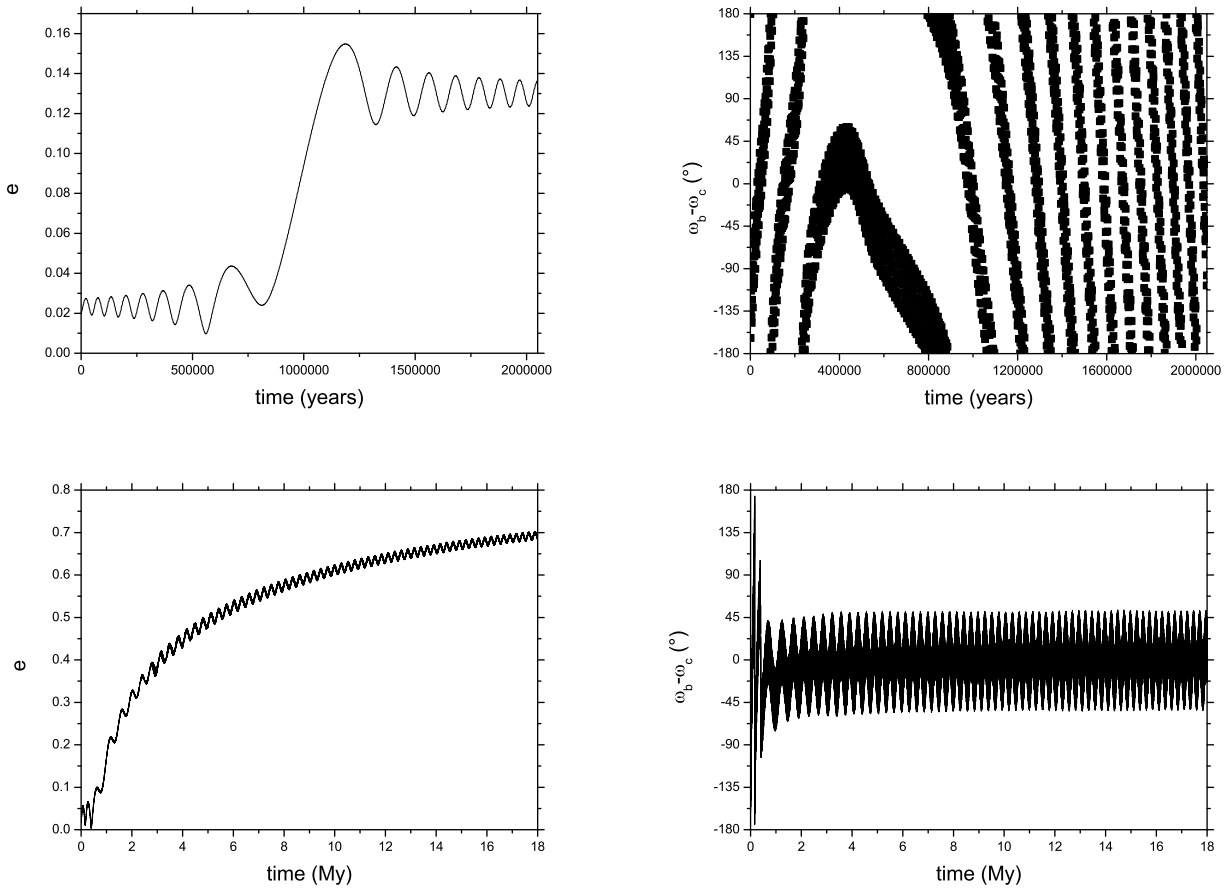


Figure 11. The sweeping of secular resonances. Top panels: Evolution of e_b when $\alpha = 1.5 \times 10^{-14}$ years in the left panel, and the related evolution of the secular angle $\varpi_b - \varpi_c$ in the right panel. Note how the angle librates during the passage of the resonance, which corresponds to a sharp increase in the orbital eccentricity of planet b . Bottom panels: Change in e_b when the spin-down parameter is smaller by 5.75% in the left plot, and the evolution of the secular angle $\varpi_b - \varpi_c$ in the right panel. This time, even if the star keeps on spinning down, planet b is locked in the resonance with planet c as a critical value for e_b is reached which generates the precession rate necessary to maintain the resonance. This causes the eccentricity of b to grow indefinitely.

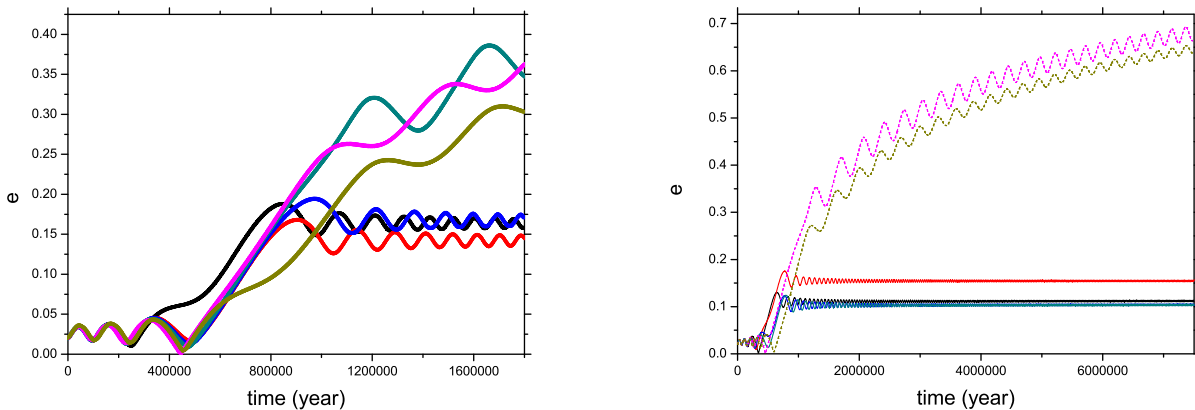


Figure 12. The growth of e_b . Left: Considering both GR and J_2 effects. Values of 10% larger and 3% and 4.5% smaller than the nominal α stabilize around a value for e_b equal to 0.15. For values of 6%, 12% and 50% smaller, e_b grow indefinitely. Right: Considering J_2 effects only. For the nominal α and values 10% larger and 9% and 15% smaller than it, e_b stabilize around 0.15. For values 22% and 50% smaller, e_b grows indefinitely.

we note that in the absence of stellar spin-down all of the configurations that we considered were dynamically stable over 10^6 years.

For completeness we consider a model with three additional terrestrial planets to see whether this promotes the sought-after instability when planet b has reached the desired eccentricity $e_b \sim 0.5$. We construct systems consisting of three additional 0.5–1 Earth-mass planets. The innermost additional body is placed 2–5 mutual Hill radii from the apocentre of the planet, calculated when its eccentricity is in the range 0.3–0.7. The second additional body is placed 2–5 mutual Hill radii from the apocentre of the first additional body, calculated when its eccentricity is in the range 0.3–0.7. The third additional planet is placed 2–5 mutual Hill radii from the apocentre of the second additional body, calculated when its eccentricity is in the range 0.2–0.7. We note that these three bodies are all placed interior 0.26 AU which is a stable zone. In fact, a planet with semi-major axis in the range 0.26 – 0.35 AU obtains a forced eccentricity $e_{\text{forced}} \gtrsim 0.2$ (see Section 2.4), which will destabilize any planets in the range 0.1 – 0.26 AU before the secular resonance is entered. We consider a spin-down parameter 5.75 % smaller than the nominal α and we calculate the necessary spin period for each case to enter resonance. We set a density of 3 g/cm³ for the additional planets and a Neptune density (1.638 g/cm³) for b . We ran more than 100 simulations, varying the planetary mutual separations.

From the results of the N-body simulations we observe that all four inner planets become involved in the resonant trapping, with the eccentricity growing for all of them before instability occurs and strong mutual interactions take place. The outcomes of these simulations include mutual close encounters, collisions between the planets, and collisions with the central star. Occasionally the inner planets can disturb the fragile resonance between the two outer giants causing catastrophic ejections from the system. Out of 100 models we find two models that replicate the present configuration with a value for $e_b \gtrsim 0.4$. When a terrestrial planet survives in the process, the model is still compatible with the detected system because, for example using the Systemic Console (Meschiari et al. 2009), a 1 Earth-mass planet at 0.19 AU would be at the noise level of the radial velocity data with an F-test value of $\approx 40\%$. Figure 14 illustrates a successful model for which only planet b survives the instabilities and is able to achieve the required eccentricity. The necessary stellar rotation period to produce the resonance is ≈ 22.2 hours. The right panel represents how all the inner planets are increasing their eccentricity during the passage of the resonance, leading eventually to close encounters and collisions which are displayed in the left panel. Orbital inclinations remain small in the system. We have tested the evolution of the systems neglecting the effects of stellar spin-down and found that the eccentricities remain small and the system is stable over runs times of 3.2 Myr.

5.2.3 The resonance with an interior planet

To test the generality of the results presented in the previous section, we evaluate how a hypothetical interior terrestrial planet may have influenced the sweeping of the resonance. We consider a single Earth-mass planet in circular orbit with semi-major axes in the range 0.03–0.055 AU. We want to as-

sess if the additional planet will be trapped long-term into the resonance with planet b (as in Sect. 5.2.2), or if its presence will release b from the resonance with the required eccentricity. We prepare a set of 100 runs with planet b initially located at 0.9–0.11 AU so that close encounters may start when a high eccentricity has already been reached. Each sub-set has its own stellar spin period for resonance capture. The particular behaviour depends on the individual run, but in general we observe that planets b and x are not quite trapped into a mutual resonance but instead experience differential precession, with the precession periods differing by approximately 2000 years. We find that collisions do occur, but because of the slow differential precession it takes on the order of 10^7 years for them to happen. Figure 15 presents a successful case: the eccentricities of the two inner planets grow because of the passage of the resonance, the orbits cross each other, after 11 Myr instability arises leading to a collision, leaving planet b with the required eccentricity. Although planet b is initiated with a semi-major axis of 0.1, the inelastic collision causes the composite planet to effectively migrate to 0.08 AU, which is the observed value. Orbital inclinations stay small in the system. To generate the resonance this simulation required a stellar rotation period $\lesssim 13.4$ hours. A set of simulations with $a_b = 0.105$ AU demands a stellar spin period of 11.3 hours. In these configurations the eccentricity stops growing and stabilizes around 0.45 as the secular resonance is disrupted.

5.2.4 Resonance passage considering stronger tidal evolution

In the previous section we showed that sweeping secular resonances due to stellar spin-down, combined with planet-planet scattering, can cause eccentricity excitation of planet b up to $e_b \simeq 0.4$, consistent with present day observations. The HD 181433 system, however, is unusual because of the large eccentricity of the inner planet in spite of the ~ 6.7 Gyr age of the star. The implication is that tidal dissipation inside the planet is weak compared with that measured for terrestrial bodies in the Solar System. If the value $e_b = 0.4$ is primordial then it implies a value of $Q_p \geq 10^5$.

A value of $Q_p \sim 10^4$ is inferred for Neptune and Uranus (Murray & Dermott 1999), and we showed in Section 3 that if such a value is adopted for HD 181433 b then the planet is approximately half-way through the process of circularising from an initial eccentricity of $e_b \simeq 0.6$ and semi-major axis $a_b = 0.1$. This raises the question of whether or not the sweeping secular resonance model with additional terrestrial-mass planets can also achieve an eccentricity this large, and we have addressed this issue below using a further batch of N-body simulations.

Here the planet b is placed further out so a shorter stellar spin period is required to generate the resonance. We infer that the star had to rotate in $\lesssim 11.0$ hours in order for the resonance to sweep the location of b . Using the nominal value of α (see equation 10) in a simulation consisting of planets b , c and d only, e_b peaks at 0.28 and stabilizes later around a value of 0.25. If we reduce the stellar spin-down rate to be equal to or less than the nominal value by just 5.75 %, e_b grows indefinitely as described above.

Our original aim was to test the possibility of breaking the secular resonance for planet b by including three addi-

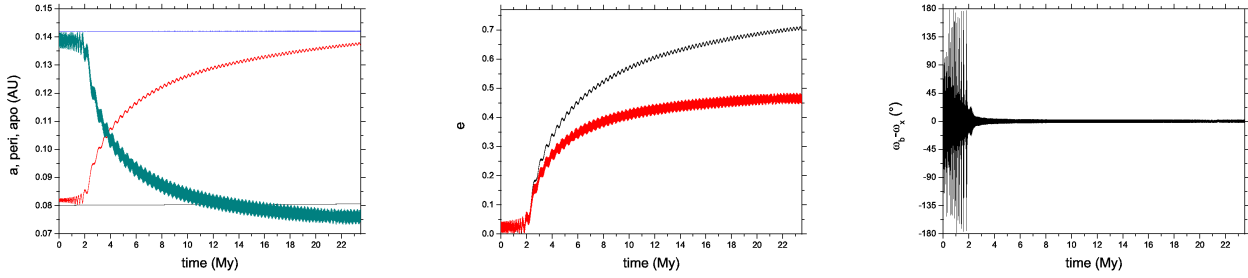


Figure 13. The process of sweeping secular resonances for HD 181433 when an Earth-mass planet is added. The spin-down parameter is reduced by 6% with respect to the nominal value. Left: Evolution of semi-major axis and apocentre for planet *b*, semi-major axis and pericentre for planet *x*. Centre: Evolution of e_b and e_x . Right: Evolution of the secular angle $\varpi_b - \varpi_x$, showing the lock into the resonance occurs after ~ 2 My.

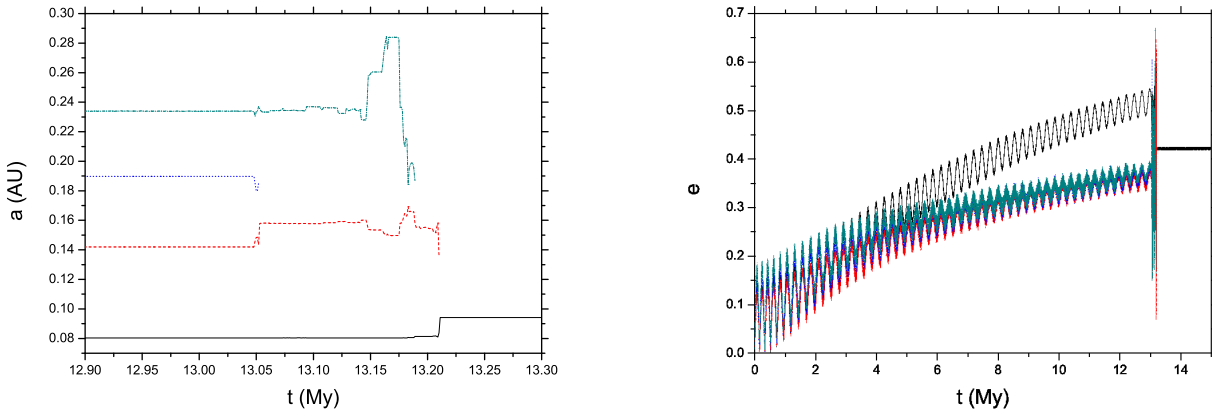


Figure 14. The sweeping of secular resonances when three extra Earth-mass planets are included in the inner part of the HD 181433 system. Left: Evolution of the semi-major axes of the four inner planets, with planet *b* being the innermost. Collisions are observed leading to reduction in the number of planets. Right: Evolution of their eccentricities, e_b is the one growing fastest, achieving a final value of 0.43.

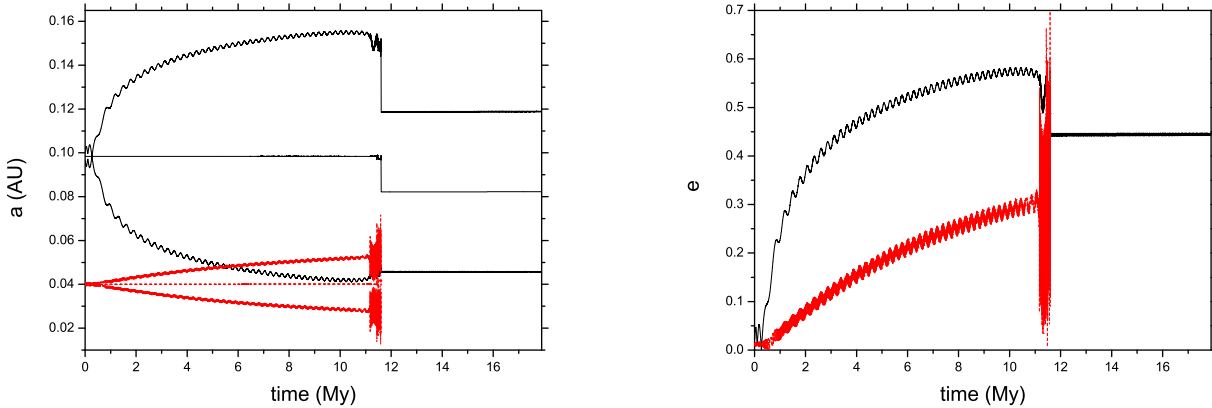


Figure 15. The passage of the resonance in the inner part of the HD 181433 system, an Earth-mass planet at 0.04 AU is included. Left: Evolution of the semi-major axes, apocentres and pericentres of the two inner planets, with planet *b* initially at 0.098 AU. The inner terrestrial planet is destroyed by collision after 11 My. Right: Evolution of the eccentricities. e_b is the one growing faster, achieving a final value of 0.44.

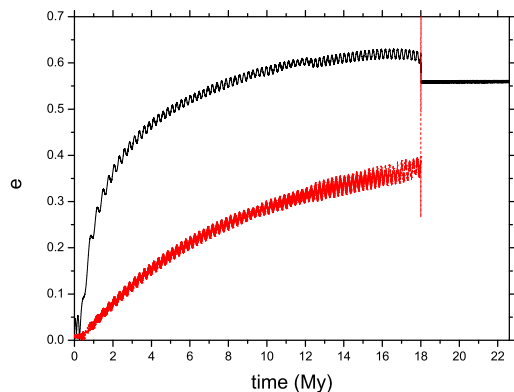


Figure 17. The passage of the resonance in the inner part of the HD 181433 system when an Earth-mass planet at 0.04 AU is included. The evolution of the eccentricities is shown with e_b growing faster and achieving a final value of about 0.56. The inner terrestrial planet is destroyed after 18 Myr.

tional terrestrial planets orbiting beyond b , but the larger initial semi-major axis and larger final eccentricity required of $e_b = 0.6$ mean that a stable system of three additional planets cannot be set-up because the outer one orbits outside the stable zone located within 0.26 AU (see Section 2 and 5.2.2). For this reason we ran a suite of simulations with two Earth-mass planets orbiting outside of planet b . The qualitative evolution is similar to that described in Section 5.2.2. An example of a successful simulation is displayed in Figure 16, showing the growth of eccentricity through secular resonance, planet-planet scattering and collision, and two surviving inner planets with planet b orbiting with $e_b \sim 0.6$ and $a_b \sim 0.1$. The necessary stellar rotation period to generate the resonance is 11.6 hours. The rocky planet which survives at 0.16 AU would be in the noise level of the measured radial velocities (F-test value of 84%). Its orbital inclination increases up to 12° for the smaller survivor while it remains much smaller for planet b . Taking account of tides with $Q_p = 10^4$, once the initially chaotic phase of evolution has finished the system will evolve to exhibit characteristics very similar to those observed today on a time scale of ~ 6 Gyr.

Note that we have tested the stability of the system without the resonance and find that it remains stable over a time-scale of 1 Myr.

Finally, we report here also an example of evolution when an Earth-mass body is placed on an orbit interior to planet b . This scenario has already been discussed in Section 5.2.3. Figure 17 shows the increase of the eccentricities for the two inner planets (b and x). Instabilities arise after 18 Myr, only planet b survives and it is left with an eccentricity $e_b = 0.56$, close to the required value. To generate the resonance a stellar rotation period $\lesssim 13.4$ hours is required.

5.3 Large forced e_b by an additional planet

The spin-down of the central star provides a means of enhancing the eccentricity of planet b . In the absence of a rapidly rotating star an additional undetected planet in the

system can also enhance the forced eccentricity of planet b by strengthening coupling with the outer giant planets. By carefully choosing of the mass and location of an additional planet the forced eccentricity of planet b may be enhanced. We focus on the effect of a low mass planet near planet b below.

5.3.1 Exterior low mass planet

Mardling & Lin (2004), for example, have investigated the hypothesis that eccentric short-period planets have eccentricities that are excited by undetected outer companions. We have already discussed in Section 2.4 that an additional planet can be stable in the region 0.1 – 0.35 AU. We use the secular model to estimate the planetary mass required in this range in order for the precession period of b to match that of c or of the hypothetical planet. We then refine the solution by means of numerical simulations, setting the eccentricities of the extra planet and b to small non-zero values and examining the evolution of 75 configurations for 10 Myr.

The maximum forced eccentricity obtained for these runs was $e_b = 0.28$ for a 12 Earth mass companion orbiting at 0.35 AU or for a 15 Earth mass companion orbiting at 0.3 AU. All other simulations have resulted in values of $e_b < 0.28$. For example, a 11 Earth mass companion orbiting at 0.25 AU resulted in a peak value of $e_b = 0.27$ (see left panel of Figure 18).

5.3.2 Interior low mass planet

We now consider the evolution when an extra planet is orbiting interior to b . We use the secular theory to estimate the planetary masses required between 0.008 – 0.062 AU for planet b to experience a significantly enhanced forced eccentricity. Results from this secular analysis indicate that an additional planet located at $a = 0.008$ AU must have a mass equal to $45 m_\oplus$. An additional planet located at $a = 0.062$ AU must have a mass equal to $0.13 m_\oplus$. Numerical integration of 40 initial configurations, covering the range of semi-major axes and m_p discussed above, show again that e_b is not forced sufficiently to explain the currently observed value of $e_b = 0.39$. The maximum forced eccentricity obtained was $e_b = 0.21$, this happened in two cases: a 1.5 Earth mass companion orbiting at 0.041 AU (right panel of Figure 18) and a 0.75 Earth mass companion orbiting at 0.056 AU.

5.3.3 Detectability

We assess the detectability of these hypothetical planets assuming a radial velocity precision of 1 m/s (Bouchy et al. 2009). In the range 0.1 – 0.35 AU planets with mass as small as 4–6 M_\oplus would be detectable. This excludes the possibility of exciting a sufficiently large e_b with an unseen planet in this region. In the inner zone, the detection limit is about 2 Earth-masses. This cannot exclude the generation of a forced eccentricity of 0.21.

If planet b had been formed with a free eccentricity of $\simeq 0.18$ then in principle the observed value of $e_b = 0.39$ could have been obtained through excitation of a forced eccentricity equal to 0.21. This value for the free eccentricity, however, is rather large for either of the two most plausible

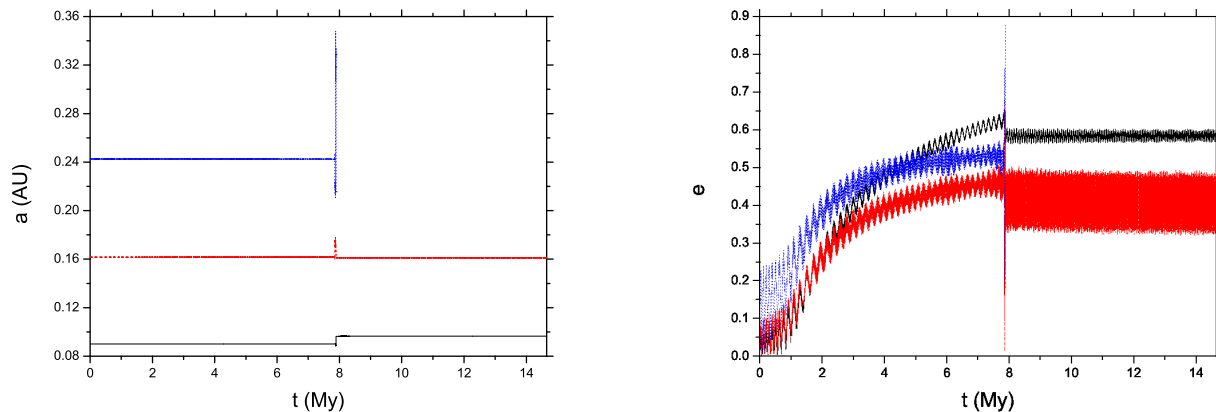


Figure 16. The sweeping of secular resonances when two extra Earth-mass planets are introduced in the inner part of the HD 181433 system. Left: Evolution of the semi-major axes of the three inner planets, with planet b being the innermost. The outer terrestrial planet is destroyed through collision after 8 My. Right: Evolution of their eccentricities. The eccentricity of the outer planet is the one growing fastest at the beginning as it is at the outer limit of the stable zone. A final value of 0.6 is achieved for e_b , while the surviving Earth-mass planet acquires an eccentricity of 0.45.

scenarios for the arrival of planet b at its current location. Gas-disc driven orbital migration of a fully formed planet b to its observed location is likely to have left the planet in an essentially circular orbit. Formation *in situ* through a series of giant impacts may have left the planet with a remnant free eccentricity, but a value of $e_b = 0.18$ requires the scattering bodies during the giant impacts phase to be approximately 6 Earth masses, which is only slightly smaller than the measured minimum mass of planet b .

6 DISCUSSION AND CONCLUSIONS

We have investigated the dynamical evolution of the three-planet system orbiting the main sequence K-dwarf star HD 181433 (Bouchy et al. 2009). The system consists of a close-in super-Earth with orbital period 9.37 days, and two sub-Jovian giant planets that orbit at much larger distance from the host star with orbital periods 975 and 2468 days. In order to be dynamically stable these outer giants need to be in a 5:2 mean motion resonance (Campanella 2011). The corresponding semi-major axes and eccentricities are $a_b = 0.08$, $a_c = 1.77$ and $a_d = 3.29$ AU. Of particular interest for our study are the large eccentricities displayed by the system: $e_b = 0.39$, $e_c = 0.27$, $e_d = 0.47$. The value for the short-period super-Earth in particular raises interesting questions that we have addressed in this paper: given the large separation between the inner super-Earth and outer giants, what are the plausible mechanisms that can lead to excitation of e_b ? Given the age of the system (~ 6 Gyr), what are the implications of the observed value of e_b for tidal evolution in the system and the Q -value for the inner body?

We assume that the HD 181433 planetary system attained its currently observed configuration shortly after dispersal of the protoplanetary disc. Analysis of the secular dynamics indicates that the eccentricity of the inner body cannot be explained through present day interactions between it and the outer giants. This analysis, however, does

point to the existence of a nearby secular resonance that could have caused eccentricity growth during earlier evolution.

The inferred mass of HD 181433b is $m_b \sin i = 7.4 M_\oplus$. If $\sin i \sim 1$ then this planet is a super-Earth. We have analysed the tidal evolution and conclude that if the tidal dissipation factor $Q_p \leq 10^3$ then tidal circularisation should be completed easily within the 6.7 Gyr age of the system. This suggests that HD 181433b is not a massive terrestrial-like planet. A value of $Q_p \geq 10^5$ leads to very little tidal evolution, implying that the system observed now is similar to its primordial state if this Q -value is appropriate. A value of $Q_p \simeq 10^4$, characteristic of Neptune and Uranus (Murray & Dermott 1999), would indicate that the system started out with $a_b \simeq 0.1$ AU and $e_b \simeq 0.6$ such that the system is essentially half-way through the tidal circularisation process. This might also indicate that HD 181433b should be considered as a hot-Neptune rather than a short-period super-Earth.

Given that all bodies in the system have quite large eccentricities, we began our study by analysing a scenario in which an additional outer giant planet was present originally, leading to global dynamical instability and ejection of this additional body. This is a natural starting point given the recent work showing that planet-planet scattering can explain the observed eccentricity distribution of the extrasolar planet population (Chatterjee et al. 2008; Jurić & Tremaine 2008). The chaotic dynamics involved in such a scenario preclude us from obtaining a close-analogue to the HD 181433 system through N-body simulations, so we restrict our analysis to addressing the following two issues as a means of estimating the likelihood that the scenario may have operated: can the short-period super-Earth be perturbed onto an eccentric orbit with the required $e_b \geq 0.4$ during the dynamical instability, given that it orbits close to the central star?; what is the likelihood of the two outer planets c and d landing in the 5:2 resonance after scattering? From a suite of 300 N-body simulations we find that e_b

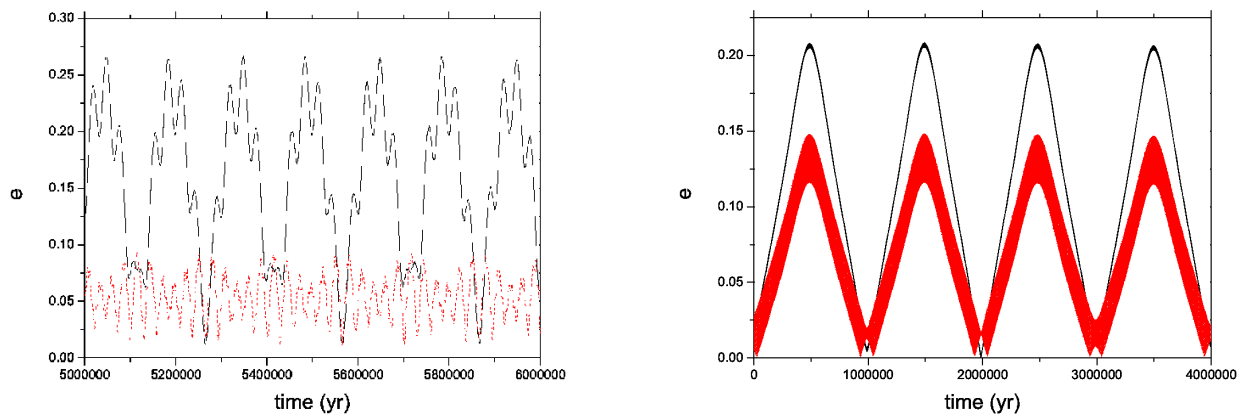


Figure 18. Eccentricity excitation. Left panel: Evolution of e_b and e_x for a case with $a_x = 0.25$ AU and $m_x = 11M_{\oplus}$. Maximum values for e_b and e_x are 0.27 and 0.09, respectively. Right panel: Evolution of e_b and e_x for a case with $a_x = 0.041$ AU and $m_x = 1.5M_{\oplus}$. Maximum values for e_b and e_x are 0.21 and 0.15, respectively.

reaches $e_b \simeq 0.4$ in 6% of the runs, and reaches $e_b = 0.6$ in 2% of them, indicating that we can obtain values of e_b that are appropriate for a range of tidal histories. Further analysis of the width of the 5:2 resonance suggests a probability for landing in resonance of $\sim 10^{-3}$, in good agreement with the more extensive set of N-body simulations of planet-planet scattering reported by Raymond et al. (2008). A naive estimate of the joint probability of eccentricity excitation for planet b and formation of the 5:2 resonance for planets c and d suggests a value $\sim 6 \times 10^{-5}$, indicating that the hypothetical planet-planet scattering scenario is plausible but only occurs as a rather rare event in planetary system evolution.

Given this conclusion regarding the planet-planet scattering scenario, we also considered the possibility that secular resonance caused excitation of planet b 's eccentricity. We examined how an additional planet in the system may have increased the secular forcing of planet b 's eccentricity, but this idea is discounted because the eccentricity obtained for masses below the detectability threshold was too small. During pre-main-sequence evolution most host stars are rapid rotators (e.g. Baxter et al. 2008). Rotational flattening introduces a J_2 component in the moments of the stellar gravitational potential. Precession caused by this effect can be important in determining the evolutionary fate of short-period planets (e.g. Ward et al. 1976; Nagasawa & Lin 2005). The semi-major axis of planet b around HD 181433 is ~ 0.08 AU, close to a secular resonance. Using customised N-body simulations that incorporate precession due to GR and stellar oblateness, and evolution of the stellar spin through magnetic braking, we have tested the hypothesis that the resonance swept past the location of b , generating the large eccentricity. We identify two distinct modes of evolution: for nominal values of the stellar spin-down parameter planet b is trapped in the resonance temporarily, leading to a maximum growth of eccentricity to $e_b = 0.25$; for values of the stellar spin-down parameter that are marginally smaller than the nominal value (i.e only 5.75% slower), planet b becomes trapped in the resonance indefinitely with its eccentricity being driven toward unity. The final fate of the system in this latter case appears to be collision with the central star.

Neither of these two outcomes leads to a system that looks like HD 181433*b*, but we find that the inclusion of additional short-period low mass planets in the system, orbiting in the vicinity of planet b , can perturb it out of long-term resonant capture when its eccentricity has reached large values. Such a scenario can account successfully for the observed orbital properties of planet b for a range of tidal histories, but in most cases we require a stellar spin period $\lesssim 20$ hours for resonant capture to occur. Given that we assume the resonant interaction occurs shortly after protoplanetary disc removal, this scenario requires that HD 181433*a* was a member of the young stellar population that displays rotation periods of less than 2 days. While these stars are in the minority, they are by no means rare (Baxter et al. 2008), suggesting that this scenario provides a plausible explanation for the high eccentricity observed for HD 181433*b*.

ACKNOWLEDGEMENTS

G.C. acknowledges the support of a PhD studentship from Queen Mary University of London. We are grateful to the referee Makiko Nagasawa for valuable comments that improved this paper.

REFERENCES

- Adams F. & Laughlin G., 2006, ApJ, 649, 1004
- Agnor, C. B., & Lin, D. N. C. 2012, ApJ, 745, 143
- Agnor C. B., Lin D. N. C., 2012, EPSC Conf., 946
- Barnes R. & Quinn T., 2004, ApJ, 611, 494
- Barker A. & Ogilvie G., 2009, MNRAS, 395, 2268
- Baxter E., Corrales L., Yamada R., Esin A., 2008, ApJ, 689, 308
- Bouchy F. et al., 2009, A&A, 496, 527
- Butler R. et al., 2006, ApJ, 646, 505
- Campanella G., 2011, MNRAS, 418, 1028
- Chambers J., 1999, MNRAS, 304, 793
- Chatterjee S., Ford E., Matsumura S., Rasio F., 2008, ApJ, 686, 580

- Christou A. A., Murray C. D., 1999, MNRAS, 303, 806
 Crida, A., Sándor, Z., & Kley, W. 2008, A&A, 483, 325
 Ford E. & Rasio F., 2008, ApJ, 686, 621
 Goldreich P. & Soter S., 1966, Icarus, 5, 375
 Gu P., Lin D., Bodenheimer P., ApJ, 2003, 588, 509
 Herbst, W., Bailer-Jones, C. A. L., Mundt, R., Meisenheimer, K., & Wackermann, R. 2002, A&A, 396, 513
 Ibgui L. & Burrows A., 2009, ApJ, 700, 1921
 Iorio L., 2005, A&A, 433, 385
 Jackson B., Greenberg R., Barnes R., ApJ, 2008, 678, 1396
 Jurić, M., & Tremaine, S. 2008, ApJ, 686, 603
 Kozai, Y. 1962, AJ, 67, 591
 Lee, M. H., & Peale, S. J. 2002, ApJ, 567, 596
 Lissauer J. et al., 2011, Nature, 470, 53
 Lissauer, J. J., Jontof-Hutter, D., Rowe, J. F., et al. 2013, arXiv:1303.0227
 Malhotra, R., Fox, K., Murray, C. D., & Nicholson, P. D. 1989, A&A, 221, 348
 Mardling, R. A., & Lin, D. N. C. 2004, ApJ, 614, 955
 Marcy, G. W., Butler, R. P., Fischer, D., et al. 2001, ApJ, 556, 296
 Mayor, M., & Queloz, D. 1995, Nature, 378, 355
 Meschiari S., Wolf A., Rivera E., Laughlin G., Vogt S., Butler P., PASP, 2009, 121, 1016
 Miller N., Fortney J., Jackson B., ApJ, 2009, 702, 1413
 Misner C., Thorne K., Wheeler J., 1973, Gravitation, W. H. Freeman and Company
 Moorhead A. & Adams F., 2005, Icarus, 178, 517
 Murray C. & Dermott S., 1999, Solar System Dynamics, Cambridge University Press
 Nagasawa M. & Lin D., 2005, ApJ, 632, 1140
 Nagasawa M., Lin D., Thommes E., 2005, ApJ, 635, 578
 Nelson, R. P., & Papaloizou, J. C. B. 2002, MNRAS, 333, L26
 Ogilvie G. & Lin D., 2004, ApJ, 610, 477
 Papaloizou, J. C. B., Nelson, R. P., & Masset, F. 2001, A&A, 366, 263
 Quinn T., Tremaine S., Duncan M., 1991, AsJ, 101, 2287
 Raymond S., Barnes R., Armitage P., Gorelick N., 2008, ApJ, 687, L107
 Skumanich, A. 1972, ApJ, 171, 565
 Snellgrove, M. D., Papaloizou, J. C. B., & Nelson, R. P. 2001, A&A, 374, 1092
 Sousa S. et al., 2008, A&A, 487, 373
 Soja R., Baggaley W., Brown P., Hamilton D., 2011, MNRAS, 414, 1059
 Torres G., Andersen J., Giménez A., 2010, A&ARv, 18, 67
 Trevisan M., Barbuy B., Eriksson K., Gustafsson B., Grenon M., Pompéia L., 2011, A&A, 535, A42
 Ward W., Colombo G., Franklin F., 1976, Icarus, 28, 441
 Ward, W. R. 1997, Icarus, 126, 261
 Winn, J. N., Fabrycky, D., Albrecht, S., & Johnson, J. A. 2010, ApJL, 718, L145